Net Energy Performance Measurements on Two Low-E Windows

J. H. Klems

Windows & Lighting Program

Applied Science Division

Lawrence Berkeley Laboratory

University of California

Berkeley, CA 94720

Abstract

Experimental studies using the Mobile Window Thermal Test (MoWiTT) Facility were undertaken to compare the performance of low-E windows manufactured with two different technologies, sputter-coated ("soft-coat") and an improved pyrolytic chemical vapor deposition ("hard-coat"). The two technologies produce coatings with different emissivities and solar absorptions. The tests showed that from the standpoint of winter average daily performance, the higher solar transmission of the pyrolytic coatings tends to offset their higher emissivity, making the average performance of windows with the two coatings more similar than one would predict on the basis of either property alone. The tradeoff between the two window types is both orientation and climate dependent. Differences between the two windows were within the small experimental uncertainty of the measurement for all orientations except south, where the pyrolytic coating produced a larger net heat gain. Summer tests in a west-facing orientation showed that both windows produced large solar heat gains if unshaded, and that shading with an interior white venetian blind was not a very effective way of reducing these heat gains.

Sponsoring Organization

This work was sponsored by the Libbey-Owens-Ford Glass Company, hereinafter refered to as the Sponsor, under Agreement No. BG90013, through the US Department of Energy under Contract No. DE-AC03-76SF00098.

Introduction

It is well known both theoretically[1] and experimentally[2] that passive solar heat gain is a significant, although frequently ignored, part of the winter energy budget for residential windows. It follows that both U-value and solar heat gain coefficient affect wintertime performance of windows, and must be considered in evaluating the energy savings

potential of improved window systems. Where improvements change only one of these properties--for example, comparing sealed-insulating glazing with and without a gas fill on one hand, or comparing clear with tinted glass on the other--it is sufficient to compare the values of the relevant property. However, low-E coatings typically produce a window system with both lower U-value and lower solar transmittance than an identical uncoated unit. In wintertime the reduced transmittance to some extent counteracts the effect of the lower U-value, and the relative size of the two effects is climate-dependent. To determine the overall effect empirically a direct measurement of net energy flow over time is necessary.

In this work the MoWiTT (Mobile Window Thermal Test) Facility[3,4] was used to compare the performance of two double-glazed sealed-insulating glass windows with different low-E coatings. The windows were intended to be identical in all other respects. The coatings chosen were a high-quality commercially available sputtered coating and a newly-available pyrolytic coating. These two deposition processes produce coatings with different chemical compositions and differing combinations of emissivity and solar transmittance. The goal of the measurements was to determine the energy performance of the two windows when measured simultaneously under a given set of weather conditions and orientations, and to compare this performance with that which would be inferred from U-value alone, since the latter is often taken as the sole meaningful measure of wintertime performance.

Samples Tested

The Sponsor supplied for testing three samples, which will be denoted Samples A, B and C. Upon receipt, each sample was permanently marked with a unique LBL identifying number (F141, F142 and F152, respectively). MoWiTT measurements were made on Samples A and B, with Sample C serving as a spare in case of breakage.

Information Provided by the Sponsor

The Sponsor made the following representations about the nature, origin and properties of the three samples: Three sputter-coated low-E, argon-filled, non-operable casement windows made by a major window manufacturer were purchased from a local supplier. One of these windows was supplied as Sample A. In the other two units the insulating glass unit was removed and disassembled. The emissivity of the sputter-coated surface was measured and found to be 0.11. This was taken to be an estimate for the emissivity of the coated surface in Sample A. Insulating glass units of the same dimensions and spacer configuration were fabricated by a subcontractor incorporating a pyrolytic coating on the number three surface in place of the sputtered coating and filled with argon using a flow-through process with oxygen sensing on the outlet gas. After filling, the insulated glass units were re-installed in the sashes, which were in turn re-installed in the frames. These two (nominally identical) units were supplied as Samples B and C. The emissivity of a sample of the glass used in the assembly of the two units was measured and determined to be 0.20, which was taken to characterize Samples B and C. Emissivity measurements were made according to the PGMC standard for hemispherical emissivity, with a spectral

coverage of 2.5 to 25 microns. In all cases the internal gas space was 0.75 inches thick, the glass thickness was 0.090 inches, and the spacer material was aluminum.

Independent Checks by LBL

LBL work was directed toward thermal characterization of the samples as supplied by the Sponsor, and accordingly there was no independent check made on the construction or procurement of the samples. However, some observations made in the course of the LBL work, as described in detail below, do serve as independent checks of some of the information supplied by the Sponsor. General inspection of the units indicated that they were nominally identical double-glazed non-operable casement windows with vinyl-clad wood frames; dimensions and frame details are shown in Figure 1. Thermographic images taken during the MoWiTT tests showed no differences in frame or edge temperatures between the two samples. Laser-raman measurements of the air content of the fill gasses for the three samples indicated that the flow-through filling process had not been effective; while Sample A had a 4.5% air concentration, Samples B and C had 73% and 83.5%, respectively. The measured overall U-values of Samples A and B are consistent with values calculated using WINDOW-3, assuming the emissivity values supplied by the Sponsor and an argon/air fill mixture determined from the laser-raman measurements. This agreement serves as a provisional verification of the coating emissivities.

Measurement Methodology

Samples A and B were mounted, as shown in Figure 2, in the two calorimeter chamber openings of the MoWiTT (Mobile Window Thermal Test) Facility, which is a mobile calorimetric facility designed to measure the net heat flow through a fenestration as a function of time under realistic outdoor conditions.[3,4] A conceptual drawing of the MoWiTT is shown in Figure 3. Consisting of dual, guarded, room-sized calorimeters in a mobile structure, the MoWiTT can simultaneously expose two windows to a room-like interior environment and to ambient outdoor weather conditions while accurately measuring the net heat flow through each window. This measurement comes from a net heat balance on each calorimeter chamber, performed at short intervals. To get an accurate net heat balance measurement and control the interior air temperature during the full diurnal cycle, each calorimeter chamber contains an electric heater, a liquid-to-air heat exchanger with measured flow rate and inlet/outlet temperatures, and a nearly continuous interior skin of large area heat flow sensors. Calibration measurements have established that the systematic uncertainty on the difference in measured net heat flows between the two chambers is less than 3 Watts. The random measurement uncertainty on the instantaneous net heat flow measured by each chamber is of the same order of magnitude, but varies with test conditions; it is estimated in the error statement presented with the measurements.

The MoWiTT was used to measure the net heat flow through Samples A and B continuously for approximately one week for each measurement period. Both summer and winter tests were done. The winter test series consisted of four measurement periods, with the MoWiTT rotated with the windows facing in a different cardinal orientation for each, to produce west-, south-, east-, and north-facing measurements. The summer test series consisted of two measurement periods in west-facing orientation. During the measurement

associated instrumentation measured a variety of internal and external conditions: An array of thermistors with radiation shields monitored the average interior air temperature in each calorimeter, and an aspirated thermistor located in the on-site weather tower measured the exterior air temperature. A standard rotating-cup anemometer and weather vane measured the free-stream wind speed and direction. A sun-tracking pyrheliometer and a horizontally-mounted pyranometer measured beam and total horizontal solar intensity, respectively. A vertically-mounted pyranometer mounted above the two window samples measured the total solar (and ground-reflected) radiation intensity incident on the windows, and a vertically-mounted pyrgeometer measured the total incident long-wave infrared radiation (emitted by the sky and ground). A specially-designed sensor located between the two window samples monitored the nighttime effective heat transfer film coefficient.

Test Conditions

Measurements were made at the MoWiTT field site located on the campus of the University of Nevada, Reno. The elevation is 4490 ft and the environs include both open fields and low-rise urban construction. The test site is shown in Figures 4 and 5.

Winter Tests

The winter tests were run during the months of January and February, 1990. Weather conditions varied during the course of the tests, with average outdoor temperature ranging from a high of 3.9 ºC (39 ºF) for the west-facing orientation to a low of -2.3 ºC (28 ºF) for the south-facing orientation. The average temperature over the entire test series was 0.7 ºC (33 ºF). The detailed outdoor temperature record is shown in Figure 6. As can be seen from the figure, daytime high temperatures range from 14º C (57º F)to -1º C (30º F) and nighttime lows range from 2º C (36º F) to -10º C (14ºF). Figure 7 shows the measured horizontal solar intensity over the duration of the test period. By comparison with Figure 6 it may be seen that while the magnitude of the day-to-night temperature swing is strongly correlated with the available solar energy, the daily mean temperature is not: Both the warmest and the coldest days were moderately sunny, while the most overcast days happened to be near the mean temperature for the entire test series. From Figure 8, which shows the site free-stream wind speed, it can be seen that the pattern is one of predominantly low wind speeds punctuated by windy periods as weather fronts move through the area. It was somewhat windy during the west-facing test (Jan. 11-18), calm during the south-facing test (Jan. 19-26), very windy during the east-facing test (Jan 26-31), and windy during the north-facing test (Feb. 3-10).

The test chamber interior air temperatures were accurately maintained at 20ºC; over the four winter test periods the mean Chamber A and Chamber B temperatures were 19.98ºC and 20.00ºC, respectively. The standard deviation of the chamber temperatures was approximately 0.15ºC, with the deviations from the mean temperature occurring principally during daytime periods of high solar gain.

Summer Tests

The summer tests were run during late August and early September. They consisted of two test periods in west-facing orientation. During the first of these (Aug. 25-30) both samples were unshaded, while during the second (Sept. 1-5) each was shaded using identical off-white interior venetian blinds adjusted to exclude direct solar rays (approximately 45º blind angle). The weather pattern during these tests was stable, as can be seen from Figures 9, 10, and 11. Daytime high temperatures were in the neighborhood of 30º C (86º F), and nighttime lows around 12º C (54º F). The days were sunny with windy afternoons and evenings followed by calm nights and mornings.

Results

Winter Tests

The key data collected by the MoWiTT is a continuous measurement of the net heat flow through the test sample for each of the calorimeter chambers. This quantity is constructed from separate and independently-calibrated continuous measurement of (1) the electrical energy delivered to the calorimeter chamber for heating, fan power and other functions, (2) the energy extracted from the chamber by a liquid-to-air heat exchanger, which is determined from measurement of flow rate, inlet and outlet temperature measurements of the heat transfer fluid, and (3) the energy flowing into or out of the calorimeter walls, which is measured by large-area heat flow meters that provide more than 90% coverage of the calorimeter surface. Each of these measurements is rapidly sampled by the computer controlling the MoWiTT, and the average value is stored periodically. For these measurements the storage occurred every 10 minutes, and the net heat flow through the test sample is constructed from the stored averages. A large number of other quantities, such as temperatures, solar flux and wind speed, are averaged and stored in the same manner. An example of the resulting net heat flow measurement is shown in Figure 12 for the west-facing measurement. It can be seen from this plot that energy flows through the two samples are quite similar.

Nighttime U-Values

The sample heat flow and temperature measurements were used to calculate the measured U-value for each 10-minute interval during the nighttime using a published method.[5] The measurements derived in this way for all four orientations were averaged together to produce the results in Table 1. This average should be the steady-state U-value for the average conditions of the test, since U is known to be a slowly-varying function of its parameters.

The computer program[6] WINDOW3.1 was used to calculate the expected U-values listed in Table 1, with the assumptions listed in the right-hand column. For both windows a wood frame of 2.4 inches average width was used, the interior temperature was taken to be 20º C and the outside temperature -1.8º C, which is the nighttime outdoor temperature averaged over the periods from which U-value data was used. Over the same time period the average exterior film coefficient was measured and found to be 10.26 ± 0.6 W/(m^2 K),

which is quite different from the WINDOW3.1 assumption. The WINDOW3.1 calculation was corrected to this film coefficient value to obtain the number given in Table 1.

We tested the gas in the sealed insulating unit of each sample for air contamination using laser-Raman spectroscopy. We found that sample A had an air concentration of (4.5 ± 0.2)% and that sample B had an air concentration of (73 ± 2)%. These tests were conducted in Berkeley in early May, 1990, some 5 months after the fabrication of sample B. After the summer tests in Reno the samples were returned to Berkeley and the air concentrations remeasured in late September, with identical results: sample A, (4.7± 0.2)%, sample B, (73± 2)%. Given that more than four months had elapsed between tests, and that both samples had in the meantime made a round trip to Reno, the agreement between the two sets of results ruled out the possibility of seal failure for either unit. Since the original intent had been to make sample B with a pure argon fill, it must be concluded that the filling method was ineffective. The calculated value in Table 1 was for the measured gas composition, as indicated.

Overall Net Heat Transfer

Three corrections were applied to data of the type shown in Figure 12 in order to produce a more accurate measurement of the net heat flow through each sample. First, a small correction was made for heat conduction through the test wall holding the sample. Second, there are occasionally spurious large deviations in the measured points caused by bursts of electronic noise, most commonly resulting from power line transients due to lightning strikes or other random phenomena. These points (of which there were on the order of zero to three per test period) were located and removed from the data. In the averaging calculations discussed below, where values are needed for each data recording period, a linear interpolation of the neighboring points was used where points had been removed. Third, during the daytime sudden changes in the solar intensity (for example, due to cloud movement) may exceed the ability of the calorimeter control system to respond rapidly. In that case, the calorimeter temperature may deviate briefly from the set point (normally by a fraction of a degree Celsius), and there is a resulting transient in the apparent net heat flow due to heat storage in the calorimeter air and the material inside the heat flow meter boundary. For example, in Figure 12 the sharp spike of negative heat flow for Sample B just before noon on January 16 is such a transient. We have previously measured the effects of such transients on the apparent net heat flow[5] and a correction was applied to each data point for this effect.

In principle, a fourth correction is necessary, since the actual interior temperatures of the two calorimeter temperatures may differ by a small amount due to imperfections in the two control systems. In practice the average temperatures of the two chambers were extremely close for all test periods, and this correction was negligible.

The resulting corrected data is shown for the four test periods in figures 13, 14, 15, and 16. Each data set was mathematically fitted with a theoretical curve of the form

$$W(t) = U \cdot A_T \cdot \Delta T(t-\delta) + F \cdot A_G \cdot I_S(t-\delta), \qquad (1)$$

where A_T and A_G are the total and glazed area of the window, respectively, W(t) is the corrected net heat flow at time t, U is the nighttime U-value determined as described above, F is the effective solar heat gain coefficient, $\Delta T(t)$ is the measured inside-outside air temperature difference at time t, $I_S(t)$ is the measured total solar flux at time t on a vertical surface at the plane of the windows, and δ is a time delay accounting for the finite response time of the calorimeter. The quantities F and δ were determined by a least-squares fit to the data. The resulting fitted curves are shown as the dashed continuous curves in Figures 13-16, and the values of F obtained are given in Table 2. The root-mean-square differences between the fitted curves and the measured values are listed in Table 3.

It is clear from Figure 12 that the net energy flows through Sample A and Sample B are not greatly different, at least in west-facing orientation. To better quantify the difference the corrected data points shown in Figures 13-16 were integrated over each 24-hour period to produce a set of daily average net heat flows. In order to limit the comparison to the effects due to the low-emissivity coatings, the data for both units were corrected to the equivalent performance with a pure argon gas fill. This correction was completely negligible for Sample A and amounted to about 6% reduction of the first term in eqn. (1) for Sample B. The resulting daily net heat flows for the winter tests are shown in Figure 17.

Summer Tests

An identical procedure was followed for the summer tests, with the resulting U-values shown in Table 4, solar heat gain coefficients shown in Table 5, and RMS differences between the measurements and the fitted curves shown in Table 6. The net heat flows corrected for transients, together with the fitted curves of Eqn. 1 from which the solar heat gain coefficients are derived, are shown in Figure 18 for the unshaded windows, and in Figure 19 for the measurements with interior blinds. The daily net heat flows are shown in Figure 20.

Discussion

Characterizing Wintertime Fenestration Performance

It is a common practice to characterize the winter performance of windows purely on the basis of U-value. The effect of doing so for the windows in these tests is shown in Figure 21, where the measured nighttime U-value for each window has been used together with the measured indoor and outdoor temperatures to calculate the average daily net heat loss. On the basis of this figure, one would be tempted to draw two conclusions: (1) Sample A is (putting aside questions of systematic measurement error, which are treated in the next section) slightly better in terms of performance (i.e., it shows a lower daily heat loss) than Sample B in all orientations, and (2) both windows impose a sizable heating load on the space, on the order of 1 KWH per day.

Comparison of Figure 21 with the measured daily net heat flows in Figure 17 shows that both of these conclusions would be wrong. In south-facing orientation, where both windows are energy gainers, Sample B outperforms Sample A. This is also the only

orientation where the performance differences between the two samples are large compared to the uncertainties in the measurements.

More importantly, however, consideration of only the thermal losses misrepresents the true performance of both windows. Far from representing a large heating load, the windows are on average nearly energy-neutral in east- and west-facing orientations, and are net energy gainers in south-facing orientation. Even in north-facing orientation, where thermal losses predominate, diffuse solar gain causes net heat loads to be significantly less (on the order of 28%) than would be predicted purely on the basis of U-value.

Because the windows were unshaded during these tests, the measured net heat flow represents the maximum amount by which actual performance could differ from that predicted from U-value alone. It is sometimes argued that solar gains should be discounted because windows will be shaded in practice, sunlight being unacceptable to occupants because it causes glare, fading of furnishings, or local discomfort. Since no winter tests with shading devices were done, it is impossible to say whether the relative winter performance of the two samples would be modified by the use of shading devices.

However, it is very unlikely that the use of shading would change the overall conclusion that consideration of U-value alone gives a misleading assessment of the windows' energy usage. During the summer tests both windows were measured with a white interior blind that had slats tilted downward at a 45º angle. In west-facing orientation this excludes direct sunlight for those hours of the day when solar gains are significant. By comparing the corresponding solar heat gain coefficients with and without blind in Table 5, it can be seen that the net effect of this interior shading device was to reduce solar gains by only about 20%. A solar gain reduction of this magnitude would not change the qualitative picture of window performance in Figure 17 for south, east and west orientations; moreover, in north orientation there is obviously no need for shading. To make the windows energy-neutral in the south-facing orientation would require a shading device that rejected some 60% of the solar gain; to make U-value alone an accurate predictor of window performance would require rejection of more than 90% of the solar gain. Since some 10% of the solar energy is absorbed in the interior pane and coating of both windows, and most of this energy goes inward, the latter is not possible for an interior shading device.

Effect of Systematic Uncertainties in the Measurements

In order to interpret correctly the measurement results presented above, it is important to recognize that the measurement process contains inherent levels of uncertainty, due to random experimental errors and the statistical nature of some of the measurement processes. In the tables we have quoted values with and additional plus-or-minus figure to represent this uncertainty. In each case the quoted "error" figure represents the standard error. Were uncertainties on calculated values are indicated, it is because there are uncertainties associated with the inputs to the calculation.

These error statements represent the inherent random errors in the measurements. However, there is a separate type of uncertainty that must be considered. The calibration of the measurement systems in the two calorimeter chambers has been ultimately established through a series of experiments, and these experiments also have a level of uncertainty.

The net result is that each chamber has a systematic uncertainty in its energy baseline of about 3 Watts. This is an uncertainty that affects all of the measurements made by a particular chamber together, that is, all measurements would move up or down by the same amount. It should be noted that on the scale of building heat loads this is a very small amount of energy flow. Over a month it would amount to some 2 KWH per window, or less than 25 cents for electric heating in a high-power-cost part of the country.

The area in which this type of uncertainty is most important is in the comparison of daily net heat flow between Sample A and Sample B. In Figure 17 it can be seen that the differences between the two samples are small; since the two samples are measured in different chambers, relative shifts in the calibration could greatly affect these differences.

In Figure 22 the differences in daily net heat flow between the two samples are compared with the level of inherent systematic uncertainty in a comparison between the two chambers. In this plot, a positive difference means that Sample B represents a smaller heating energy cost to the building (or a greater energy gain) than Sample A, and conversely for a negative difference. The effect of the systematic uncertainty is to make the location of the zero line in this plot uncertain over the range indicated by the two dotted lines. When this uncertainty is taken into account, it is clear that the measurements cannot unambiguously demonstrate that one of the samples is better or worse than the other, except in the case of south-facing.

This systematic calibration uncertainty results in an additional U-value uncertainty of 0.13 W/m^2 K for each of the measured values in Tables 1 and 3, which for the winter tests is larger than the random measurement uncertainty. When this uncertainty is taken into account, it is clear that the measured U-values are consistent with the expected values for both samples.

For the solar heat gain coefficient measurements systematic uncertainty is a small effect, since daytime solar gains are typically large compared with 3 Watts. For the values in Tables 2 and 4, systematic uncertainty is less than 1% except for the case of winter North-facing tests, where it is on the order of 3%.

How Representative Are the Test Conditions?

It must be stressed that daily net heat flow as shown in Figures 17 and 20 is strongly climate and orientation dependent, since it represents the difference between thermal heat loss and solar heat gain. The trend in performance differences visible in Figure 20 is both significant and understandable from the U-Value and Solar Heat Gain Coefficient measurements in Tables 1 and 2: Sample B has both a higher U-Value and a higher Solar Heat Gain Coefficient than Sample A; thus, Sample B will tend to perform better when solar gains are high, while the relative performance of Sample A will improve when outside temperatures are low and overcast conditions make solar gains low.

This leads to the question, to what extent does the fact that the tests were conducted at a particular location limit the usefulness of the daily net heat flow data?

If we integrate Equation 1 over a 24-hour period, on the left-hand side we obtain the daily average net heat flow, while on the right-hand side we obtain for the two independent variables the total number of heating degree-hours in the day (W-h/day, relative to the

interior chamber temperature of 20ºC, or 68ºF) and the total daily solar flux (W-h/[m^2 day]) incident on a vertical surface, respectively. Since, as is demonstrated by Figures 13-16, Equation 1 provides an adequate explanation of the measured net heat flow, these two independent quantities may be taken as determining the daily net heat flow.

To examine the degree to which the measurement conditions are location-specific, we can compare the measured values of these two variables with values derived from average January weather conditions in other locations around the U.S. If we averaged the data over all four test periods, it is clear that we would obtain a number not too different from the average condition for Reno in January, which, while cold, is considerably sunnier than many other U.S. locations. However, we have measurements for a series of particular days, and it is not necessary to average them. The conditions of a particular 24-hour test day (for example, a cold, cloudy day) may be much more similar to the average conditions in some other location than they are to the Reno average, and in this way measurements at a particular location may utilize weather variations to produce results applicable to a variety of locations.

In Figure 23 the number of daily heating degree hours is plotted verses the daily integrated vertical-surface solar flux at the window for each measurement day. For comparison, the average January values are also plotted for four locations: Reno, NV; Washington, DC; Madison, WI; and Boston, MA. The average vaues were obtained from National Weather Service data.[7-9] For each location , points are plotted for north-, south-, east-, and west-facing orientations. It can be seen from the figure that the test days include the range of conditions characteristic of January in Washington, DC or Boston, MA, but do not include the combination of cold conditions and low solar gain characteristic of Madison, WI.

New Information Provided by these Measurements

The MoWiTT measurements described in this report provide information about the samples beyond what can be obtained through laboratory tests in three areas: (1) measurements of the window thermal properties (U-value and solar heat gain coefficient) under actual outdoor conditions rather than laboratory standard conditions, (2) a check, as in Figures 13-16 of how well the model utilizing these property vaues predicts the measured heat flow, (3) direct measurements of the daily net heat flow for particular sets of outdoor conditions.

In Tables 1 and 4 the expected U-values listed are those expected under the measurement conditions, so nearly as they can be approximated using WINDOW 3.1. This means that the calculation was made for temperatures corresponding to the average nighttime conditions, and that an explicit film coefficient correction was made to the WINDOW 3.1 result to account for the measured exterior heat transfer coefficient, since it is known that the program does not predict exterior film coefficients correctly. Under the ASHRAE standard winter conditions the WINDOW 3.1 prediction for Sample A is 2.02 W/m^2K as compared with the expected value under field conditons of 1.70 ± .02 W/m^2K listed in Table 1. The standard condition value for Sample B is 2.25 W/m^2K as compared with the Table 1 value of 1.88 ± .02 W/m^2K. While the effect of the exterior film coefficient on the calculation is small, since these are both high performance windows, it is still large compared either to the difference between the two units or the experimental uncertainty.

For the summer tests the corresponding values were Sample A, value under standard conditions 1.86 W/m^2K as compared with a Table 4 value of 1.77 ± .01 W/m^2K; Sample B, value under standard conditions 2.14 W/m^2K as compared with a Table 4 value of 1.97 ± .01 W/m^2K. Note that summertime conditions are not favorable for measuring U-value because of the small temperature differences; hence the relatively large experimental errors quoted.

The degree to which the model of equation 1 matches the data is quantified in Tables 3 and 6, which list the root-mean-square difference between the measured net heat flow and that calculated with equation 1 using the fitted values of U and F. This quantity measures the degree of mismatch between the theoretical curve and the measured data. It can be seen that the model does best for north-facing orientation and worst for south-facing, with east- and west-facing intermediate between the two. From Figure 14 it can be seen that the daytime curves do not quite reach the peak measured values on high solar gain (i.e., clear) days. This may be due to the use of a single average value for F; and angle-dependent F, as would be expected on first principles, would tend to produce a somewhat narrower effective daytime shape to the theoretical curve, and might achieve a better fit . One would expect a non-angle-dependent F to work best for north-facing, as is observed.

Conclusions

Solar gain was an important determinant of the winter thermal performance of both window samples. Average performance calculations based only on U-value significantly overpredicted winter heat loss even for north-facing orientation, and for other orientations completely distorted the thermal performance picture, e.g., predicting a heat loss when in fact there was on the average a net heat gain.

Differences in average daily winter performance between Sample A and Sample B were not significant relative to the measurement uncertanties for any orientation except south-facing, where Sample B was significantly better. The measurement uncertainties correspond to very small heat flows in any practical sense.

Measured trends in performance, which were significant, indicate that south-facing orientations and/or mild climates tend to favor Sample B's winter performance, while north-facing orientations, low average solar availability, and/or cold climates tend to shift the balance toward Sample A. This is in agreement with what one would expect from a simple model of the performance of the two windows. True relative performance, however, should only be determined from detailed calculations taking into account orientation, temperature, solar availability, and the utilizability direct solar gain.

The higher solar transmittance of Sample B becomes a liability during the summer; however, in the unshaded summer tests the difference in heat gains between the two windows was much smaller than the solar heat gain of either window. Neither window would be suitable without shading in an orientation receiving direct sunlight if cooling load or thermal comfort were an issue.

Interior shading was not very effective at reducing solar heat gain for either window.

In general both windows were well-described by a simple heat transfer model utilizing two constants, U-value and solar heat gain coefficient, to describe the window properties.

However, the values of these two constants that best fit the measurements were not those that would be measured or calculated under standard conditions.

The U-values predicted by WINDOW3.1 for the specific measurement conditions did not include the correct value for the exterior film coefficient. Once explicit correction for exterior film coefficient was made, there was reasonable agreement between the measurements and the WINDOW3.1 calculations.

The WINDOW3.1 predictions of shading coefficient, which are for normal incidence, did not agree with values of effective shading coefficient obtained from the measurements. The agreement was best for the summer west-facing data, where the intensity-weighted solar incident angle is closest to normal incidence. The dependence of effective solar heat gain coefficient on window orientation indicates that WINDOW3.1 values should not be considered synonymous with effective solar heat gain (or shading) coefficient and used directly to calculate energy performance.

References

1. Berman, S. M. and Silverstein, S. D., "Energy Conservation in Window Systems", in *Efficient Use of Energy* 285-299 (American Institute of Physics, New York, 1975).
2. Klems, J. H., *ASHRAE Trans.* **95** (1), 609 (1989).
3. Klems, J. H. , Selkowitz, S. and Horowitz, S., "A Mobile Facility for Measuring Net Energy Performance of Windows and Skylights," in *Proceedings of the CIB W67 Third International Symposium on Energy Conservation in the Built Environment* 3.1 (An Foras Forbartha, Dublin, Ireland, 1982).
4. Klems, J. H., *Journal of Solar Energy Engineering* **110**, 208 (1988).
5. Windows and Daylighting Group, *WINDOW 3.1* (Lawrence Berkeley Laboratory, Berkeley, CA, Report no. LBL-25686, 1988).
6. Crow, Loren W., "Weather Year for Energy Calculations", *ASHRAE Journal* 42 (June, 1984).
7. SOLMET, Vol. 1, User's Manual, Department of Energy Contract No. (49-26)-1041 (U. S. Department of Commerce, Asheville, NC, 1978).
8. SOLMET, Vol. II, Final Report, Department of Energy Contract No. (49-26)-1041 (U. S. Department of Commerce, Asheville, NC, 1979).

Acknowledgement

The facility used in this work was developed with support from the Assistant Secretary for Conservation and Renewable Energy, Office of Building and Commercial Systems, Building System Division, U. S. Department of Energy under contract no. DE-AC03-76SF00098.

Table 1. Nighttime U-Values from Winter Tests			
	Measured $W/(m^2 K)$	Expected $W/(m^2 K)$	Calculation Assumptions
Sample A	1.73 ± .03	1.70 ± .02	Low-E Emissivity=0.11 Fill: 95.5% Argon , 4.5% air
Sample B	2.00± .04	1.88 ± .02	Low-E Emissivity=0.20 Fill: 27% Argon, 73 % air

Table 2. Winter Solar Heat Gain Coefficients and Shading Coefficients				
Conditions	Sample A		Sample B	
	Solar Heat Gain Coefficient	Shading Coefficient	Solar Heat Gain Coefficient	Shading Coefficient
West-facing	.510 ± .004	.593 ± .005	.562 ± .004	.653 ± .005
South-facing	.562 ± .003	.653 ± .003	.649 ± .002	.755 ± .002
East-facing	.485 ± .003	.564 ± .003	.550 ± .002	.640 ± .002
North-facing	.441 ± .009	.513 ± .010	.492 ± .008	.572 ± .009
WINDOW 3.1 Calculation		.777		.869

Table 3. Root-Mean-Square Difference Between Measured and Calculated Net Heat Flow, Winter Data

Conditions	Sample A (Watts)	Sample B (Watts)
West-facing	19	22
South-facing	52	48
East-facing	17	25
North-facing	6	8

Table 4. Nighttime U-Values from Summer Tests

	Measured $W/(m^2 K)$	Expected $W/(m^2 K)$	Calculation Assumptions
Sample A	1.70 ± .43	1.77 ± .01	Low-E Emissivity=0.11 Fill: 95.5% Argon , 4.5% air
Sample B	1.77± .21	1.97 ± .01	Low-E Emissivity=0.20 Fill: 27% Argon, 73 % air
Sample A with Interior Blind	1.49 ± .56		
Sample B with Interior Blind	1.52 ± .21		

Table 5. Summer Solar Heat Gain Coefficients and Shading Coefficients

Conditions	Sample A		Sample B	
	Solar Heat Gain Coefficient	Shading Coefficient	Solar Heat Gain Coefficient	Shading Coefficient
No Blind	.641 ± .005	.737 ± .006	.720 ± .005	.828 ± .006
Interior Blind	.510 ± .003	.586 ± .004	.584 ± .003	.671 ± .004
WINDOW 3.1 Calculation No Blind		.777		.869

Table 6. Root-mean-square Difference Between Fitted Curve and Measured Net Heat Flow, Summer Data

Conditions	Sample A (Watts)	Sample B (Watts)
No Blind	31	38
White Interior Blind	27	35

Figure Captions

1. (a) Overall appearance and dimensions of the test windows; (b)frame cross section.

2. The test samples mounted in the MoWiTT calorimeter chambers. Sample A is on the right in the photograph. The narrow window-like object in the center is a device for monitoring the effective exterior film coefficient. Shown at top are the vertically-mounted pyranometer and pyrgeometer that measure the incident solar flux and the effective radiant temperature, respectively.

3. A schematic drawing of the MoWiTT facility indicating some of its key features.

4. The MoWiTT facility at its test site at the experimental farm of the University of Nevada, Reno. The MoWiTT is shown together with its auxiliary service trailer and on-site weather tower. In this photo the MoWiTT is in south-facing orientation. One can see the general conditions of the site and the environs to the north. The equipment and small trees in the foreground are at some distance from the facility and do not obstruct either solar or wind incident on the windows, although they may of course create local wind turbulence.

5. A view of the MoWiTT in north-facing orientation showing its southern environs, which include downtown Reno The large building appearing immediately behind the MoWiTT is separated from the facility by a wide field and Interstate 80.

6. The measured outdoor air temperature during the winter tests.

7. The measured solar intensity incident on a horizontal surface during the winter tests.

8. The wind speed as measured at the on-site weather tower during the winter tests.

9. The measured outdoor temperature during the summer tests.

10. The measured horizontal-surface solar intensity during the summer tests. The smooth curves such as on September 27 and 30 indicate clear or uniformly hazy conditions; rough curves such as on September 26 indicate partly cloudy conditions.

11. The measured on-site wind speed during the summer tests.

12 Sample Net Heat Flow--West facing. The total net heat flow through the sample, derived from the calorimetric measurements, as a function of time. Positive heat flow denotes heat gain; negative, heat loss. The sharp negative-going spike on January 16 for Sample B is due to a transient instrumental effect, and is not a valid heat flow measurement; those points were eliminated from subsequent data analysis, as explained in the text.

13. A comparison between the measured (points) and calculated (curve) values of the net heat flowing through each window, as a function of time, for each sample during the west-facing winter test period. The curves were generated using equation 1 and the fitted parameter values as discussed in the text. The measured net heat flow has been corrected for transient heat storage in the calorimeter chambers and flanking heat loss through the sample-holding frame.

14. A comparison between the measured (points) and calculated (curve) values of the net heat flowing through each window, as a function of time, for the south-facing winter test period. The curves were generated using equation 1 and the fitted parameter values as discussed in the text. The measured net heat flow has been corrected for transient heat storage in the calorimeter chambers and flanking heat loss through the sample-holding frame.

15 A comparison between the measured (points) and calculated (curve) values of the net heat flowing through each window, as a function of time, for the east-facing winter test period. The curves were generated using equation 1 and the fitted parameter values as discussed in the text. The measured net heat flow has been corrected for

transient heat storage in the calorimeter chambers and flanking heat loss through the sample-holding frame.

16. A comparison between the measured (points) and calculated (curve) values of the net heat flowing through each window, as a function of time, for the north-facing winter test period. The curves were generated using equation 1 and the fitted parameter values as discussed in the text. The measured net heat flow has been corrected for transient heat storage in the calorimeter chambers and flanking heat loss through the sample-holding frame.

17. A comparison of the daily net heat flowing through each sample during the winter tests. The measured data in Figures 13-16 were averaged over each 24-hour period, with corrections as explained in the text.

18 A comparison between the measured (points) and calculated (curve) values of the net heat flowing through each window, as a function of time, for the west-facing summer test period with both windows unshaded. The curves were generated using equation 1 and the fitted parameter values as discussed in the text. The measured net heat flow has been corrected for transient heat storage in the calorimeter chambers and flanking heat loss through the sample-holding frame.

19. A comparison between the measured (points) and calculated (curve) values of the net heat flowing through each window, as a function of time, for the west-facing summer test period with both windows shaded by a white interior venetian blind with slats tilted at 45º. The curves were generated using equation 1 and the fitted parameter values as discussed in the text. The measured net heat flow has been corrected for transient heat storage in the calorimeter chambers and flanking heat loss through the sample-holding frame.

20. A comparison of the daily net heat flowing through each sample during the summer tests. The data was derived as in Figure 17.

21. A calculation of the average daily net heat flowing through each window during the winter tests, utilizing only the measured U-value and indoor-outdoor temperature difference.

22. The difference between the Sample B and Sample A net heat flows in Figure 17, compared with the estimated magnitude of the systematic (baseline) uncertainty in the measurements.

23. The measurement climatic conditions compared with normal conditions for different orientations in various locations. For each test day, the measured number of heating degree-hours for the 24-hour period is plotted against the total integrated vertical-surface solar flux (open circles). Average January conditons for four locations (other symbols) are plotted for comparison. For each of the four locations there are four points, corresponding to four assumed orientations of the window.

(a)

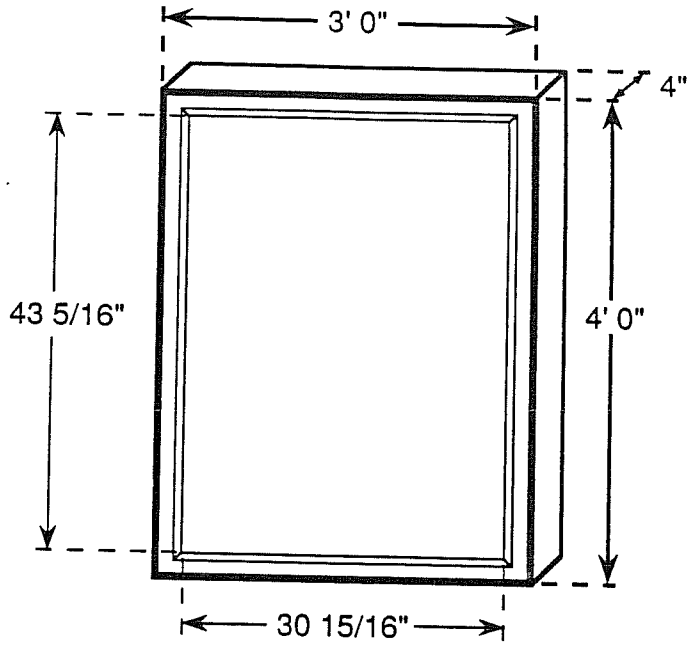
3' 0"
4"
43 5/16"
4' 0"
30 15/16"

(b)

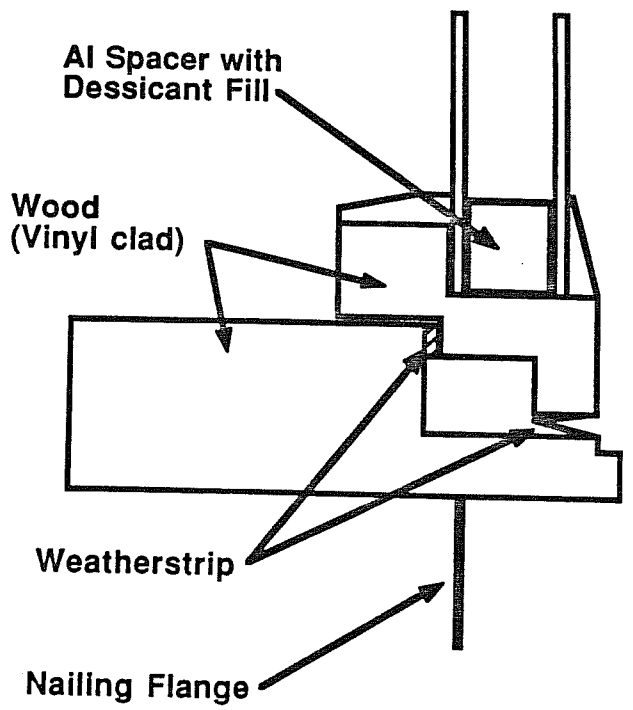
Al Spacer with
Dessicant Fill
Wood
(Vinyl clad)
Weatherstrip
Nailing Flange

Fig 1

Fig 2
BBC 905-4487
get B&W photo

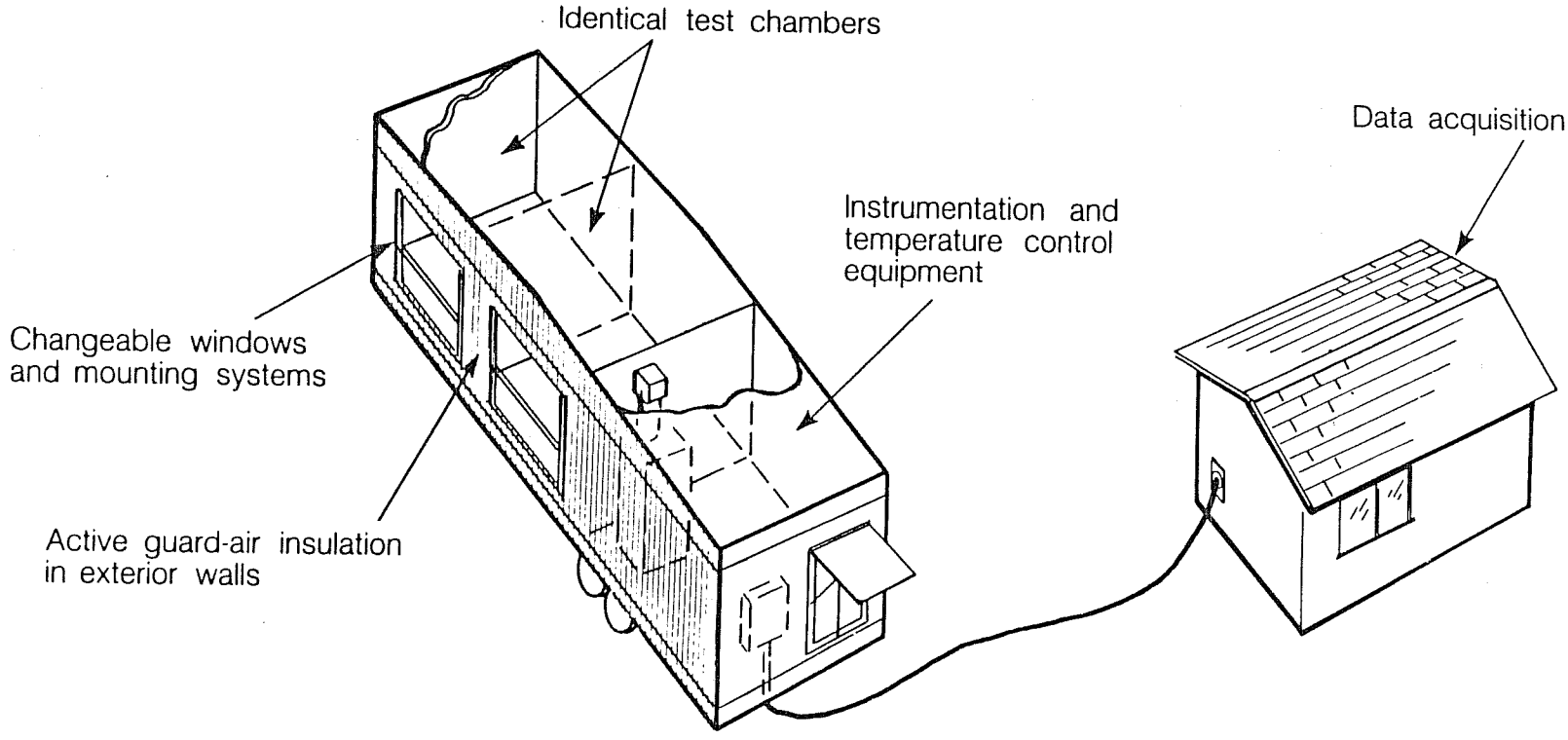

XBL 894-6908

Fig 3

Fig 4
CBB-860-10756
get B&W photo

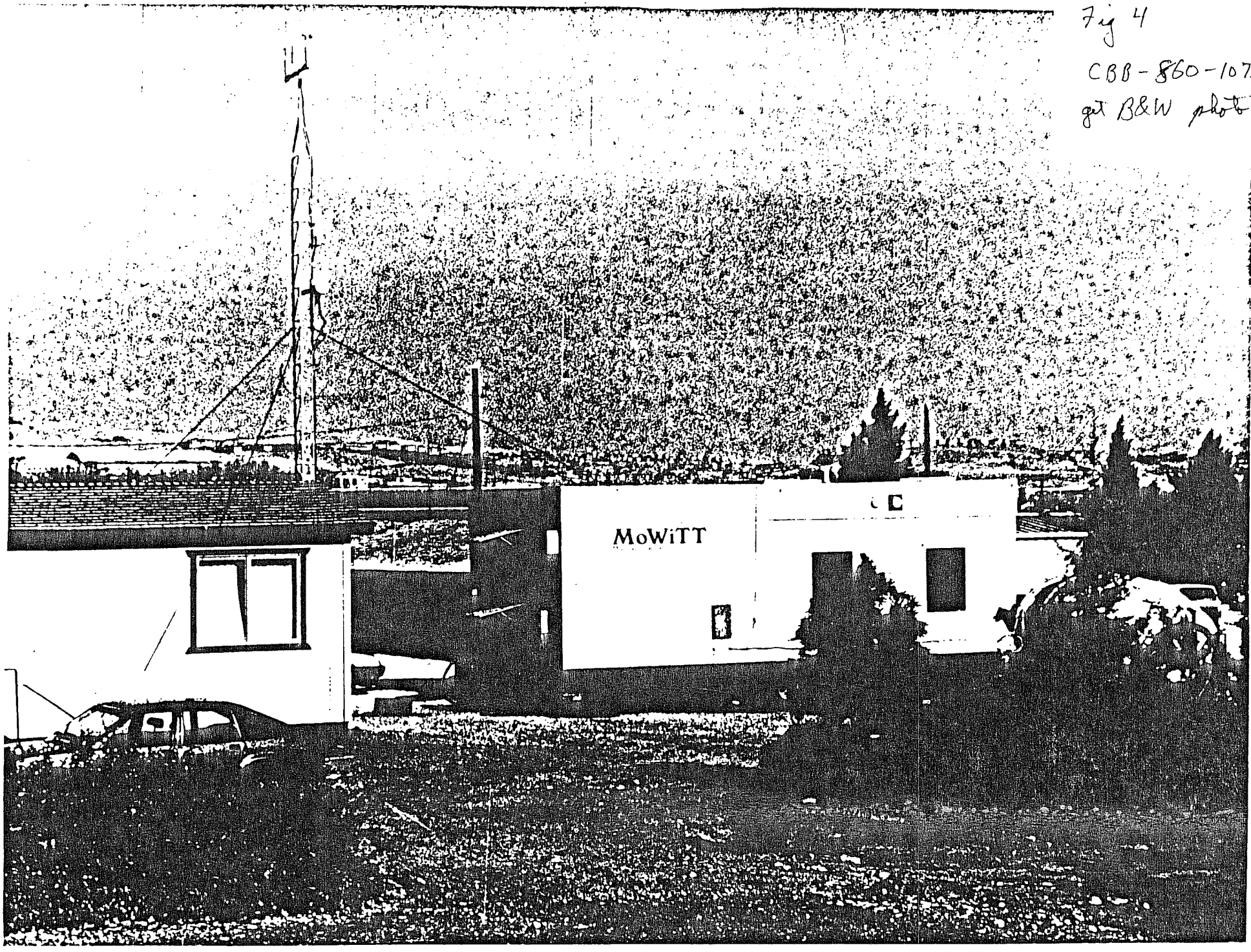

Fig 5
CBB 892-813A
get B&W photo

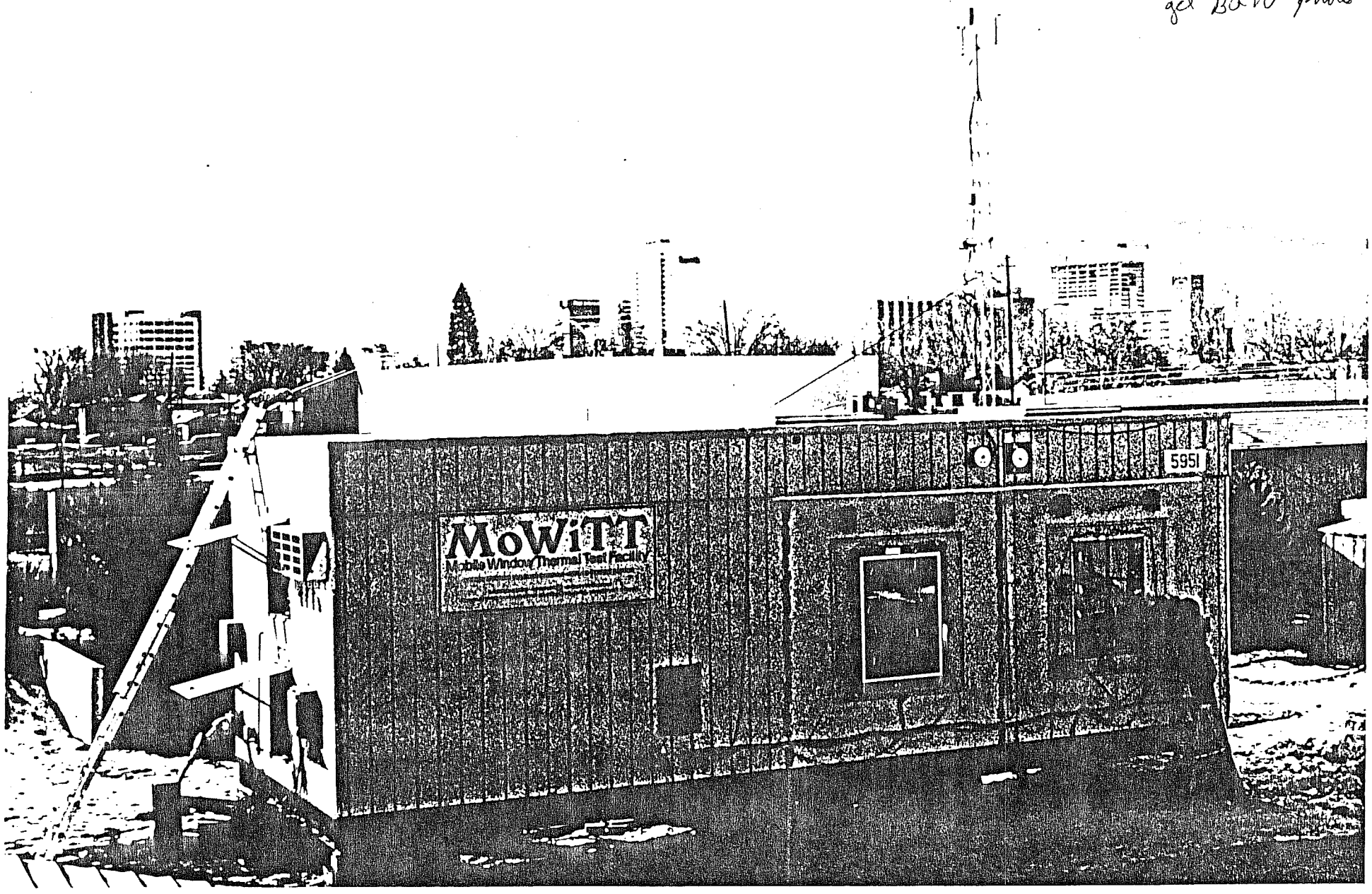

Fig 6

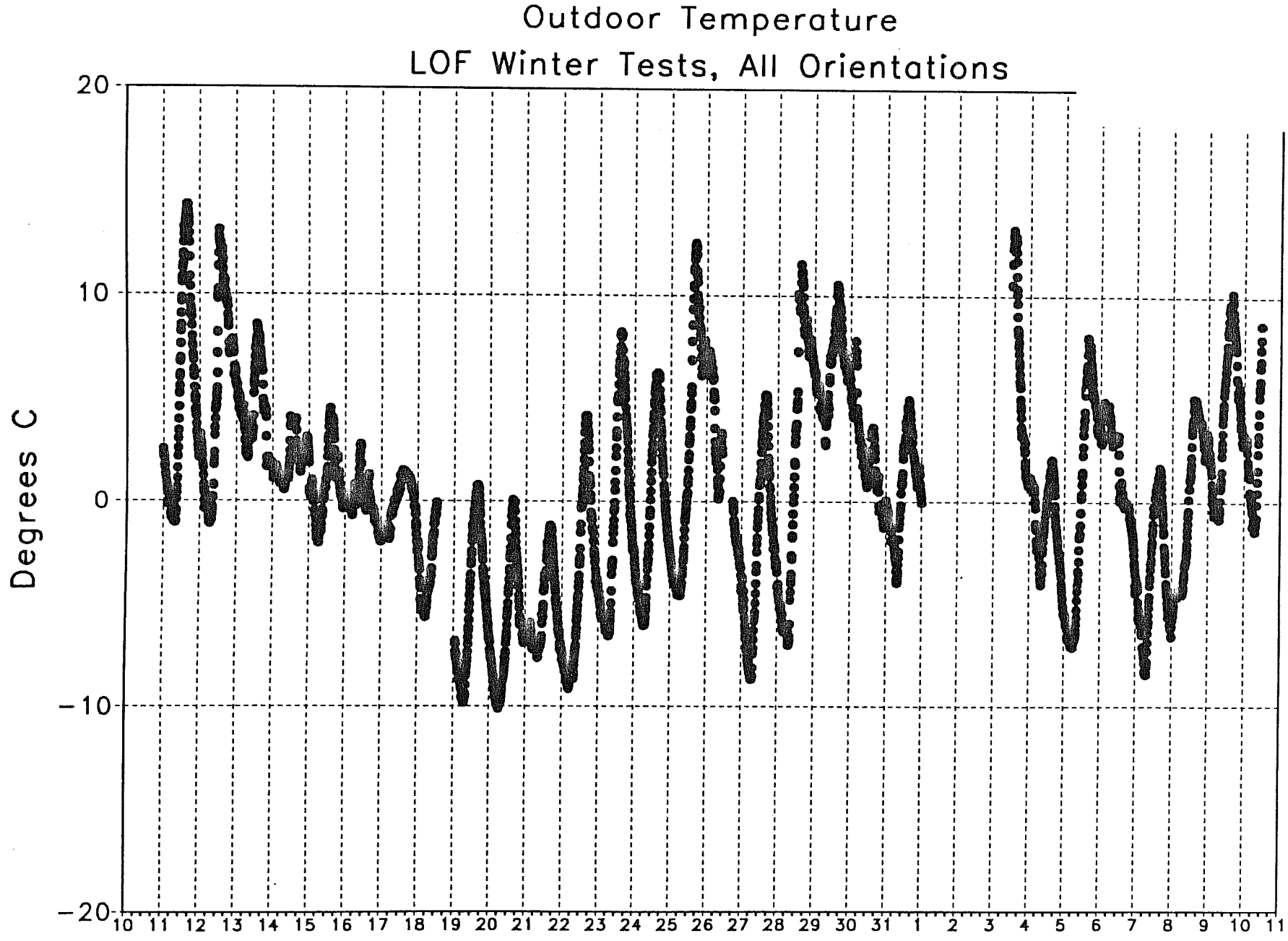

3279142692

Fig 7

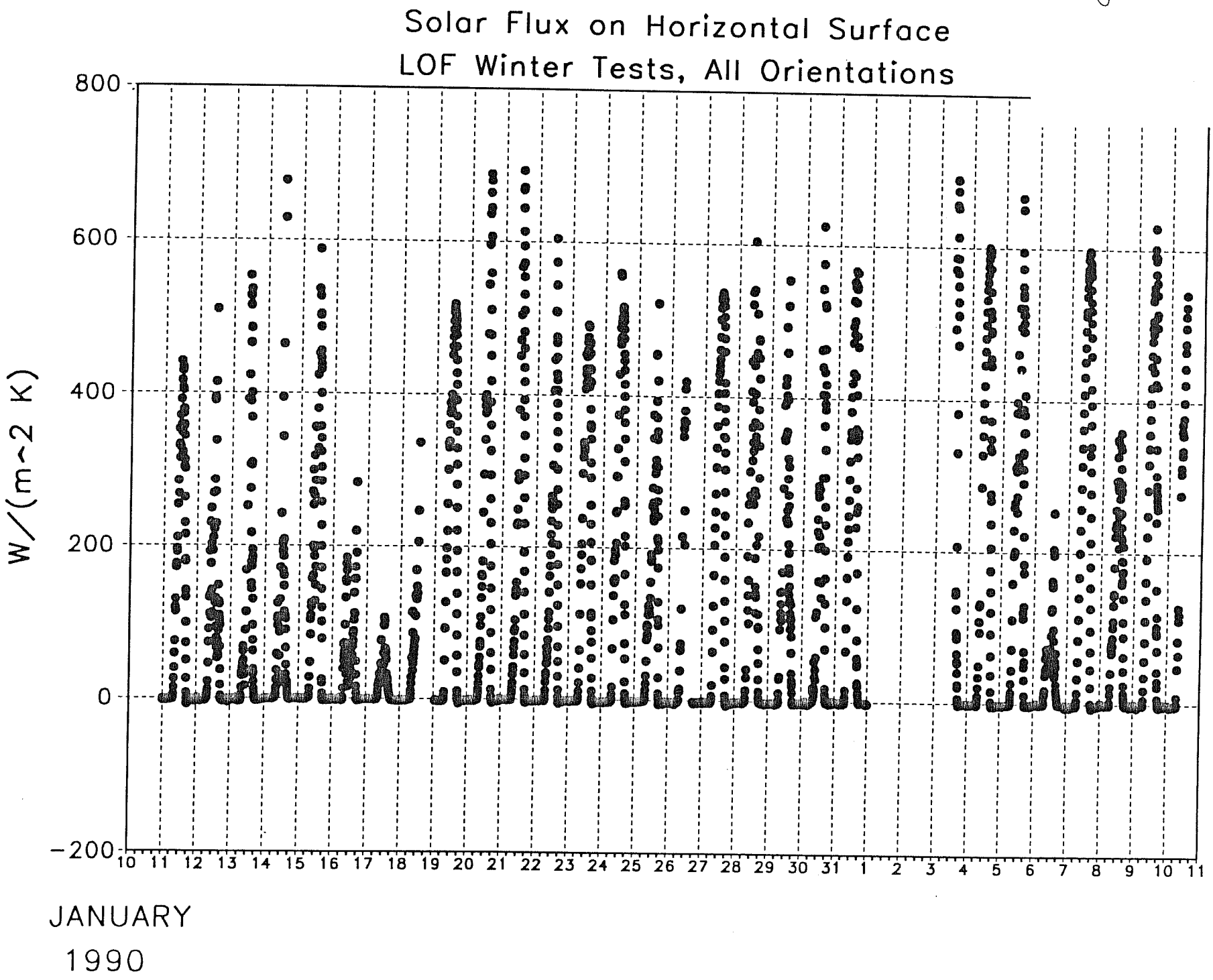
Solar Flux on Horizontal Surface
LOF Winter Tests, All Orientations
800
600
400
200
0
-200
W/(m^2 K)
10 11 12 13 14 15 16 17 18 19 20 21 22 23 24 25 26 27 28 29 30 31 1 2 3 4 5 6 7 8 9 10 11
JANUARY
1990

42692

Fig 8

Site Wind Speed
LOF Winter Tests, All Orientations

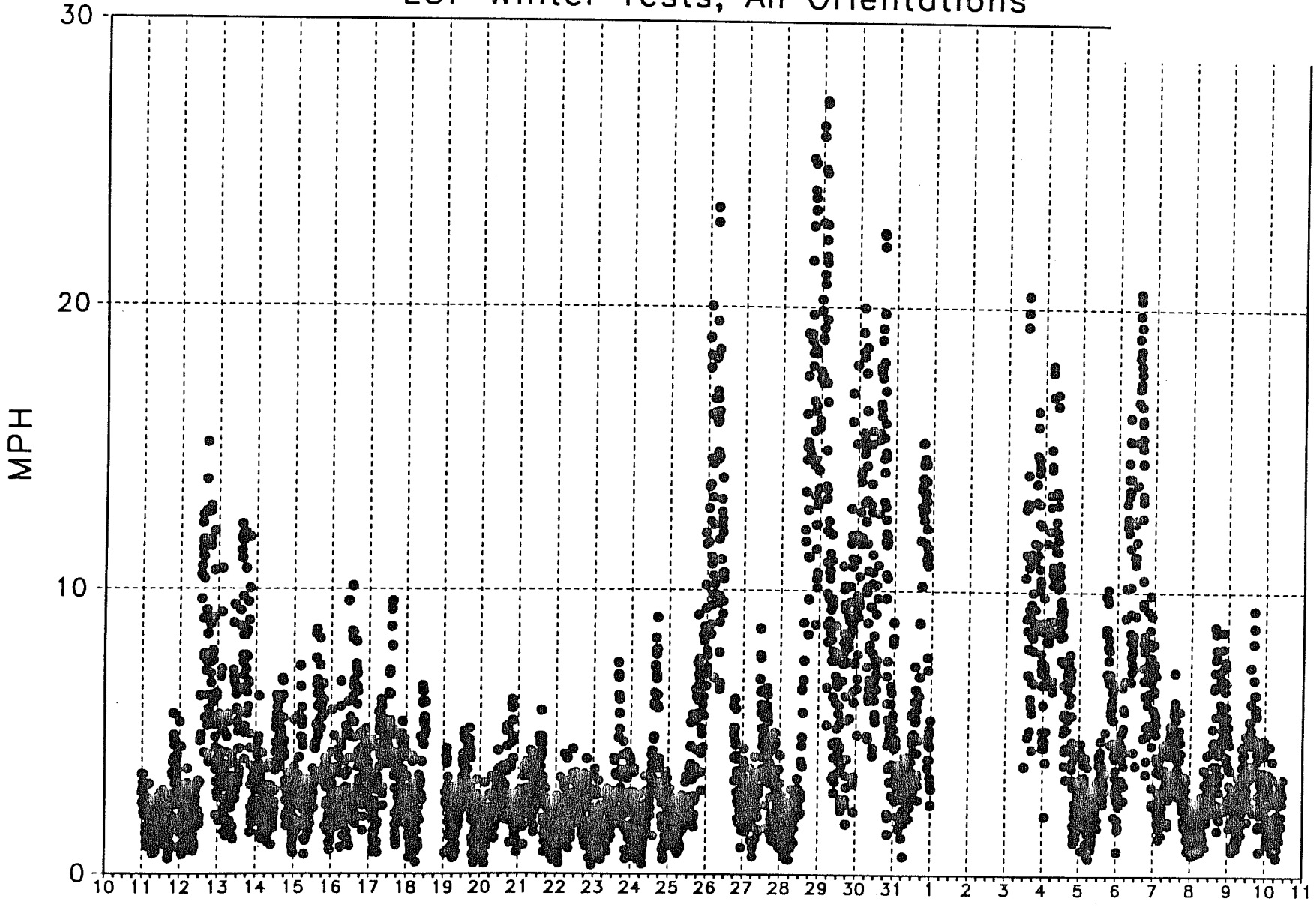

42692

Fig 9

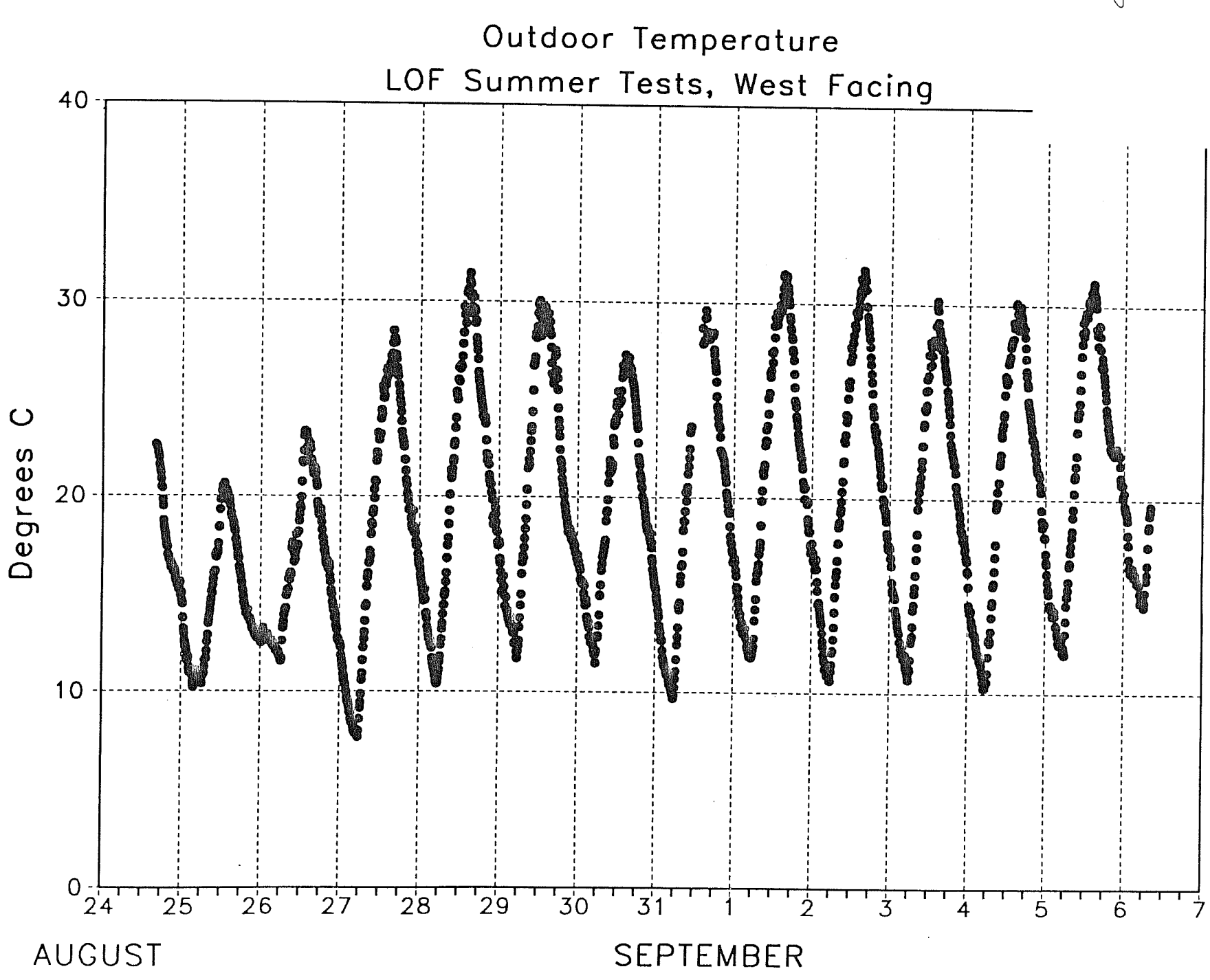
Outdoor Temperature
LOF Summer Tests, West Facing
Degrees C
40
30
20
10
0
24
25
26
27
28
29
30
31
1
2
3
4
5
6
7
AUGUST
SEPTEMBER
1990

Fig 10

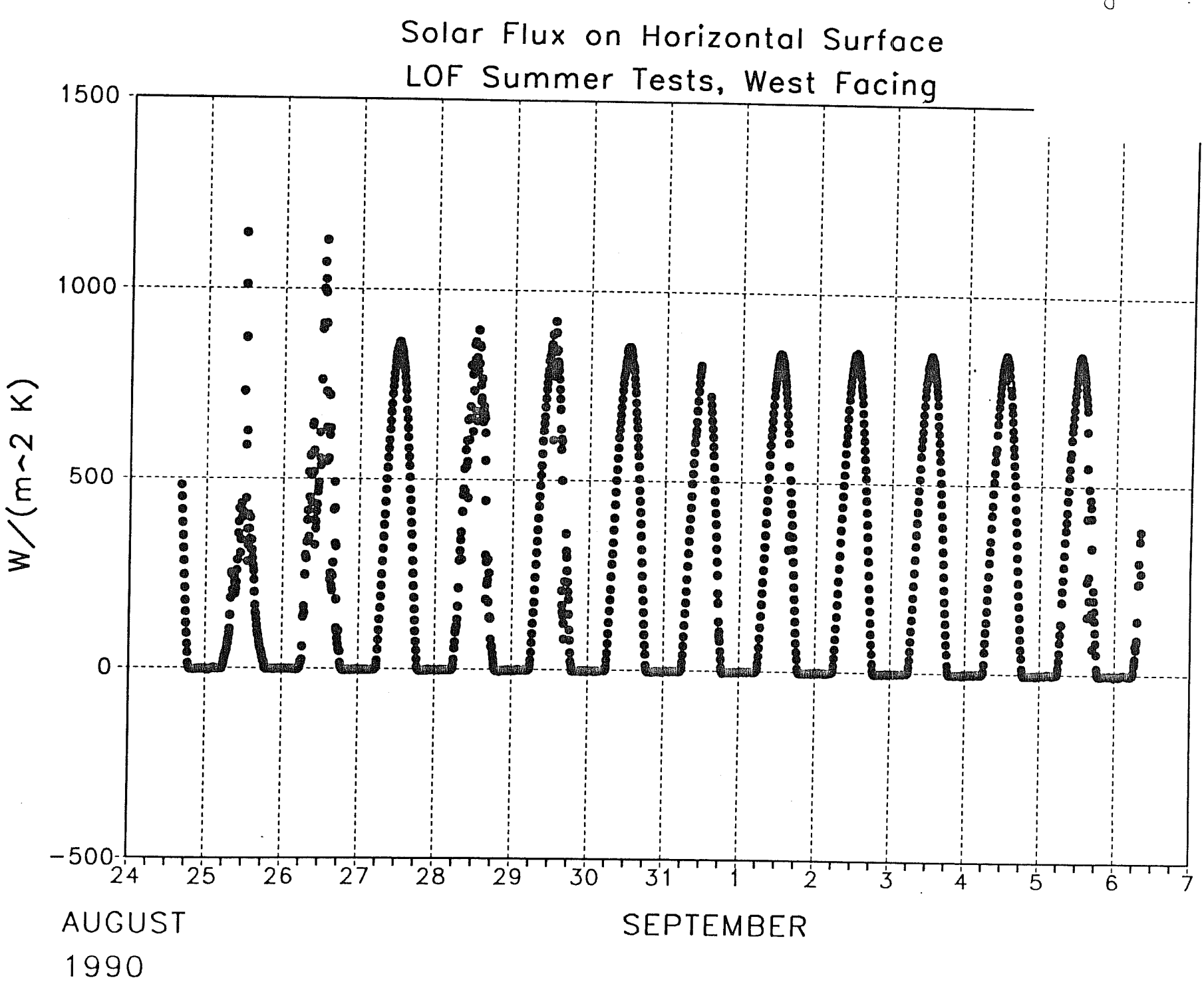
Solar Flux on Horizontal Surface
LOF Summer Tests, West Facing
1500
1000
500
0
-500
W/(m~2 K)
24
25
26
27
28
29
30
31
1
2
3
4
5
6
7
AUGUST
1990
SEPTEMBER

43059

Fig 11

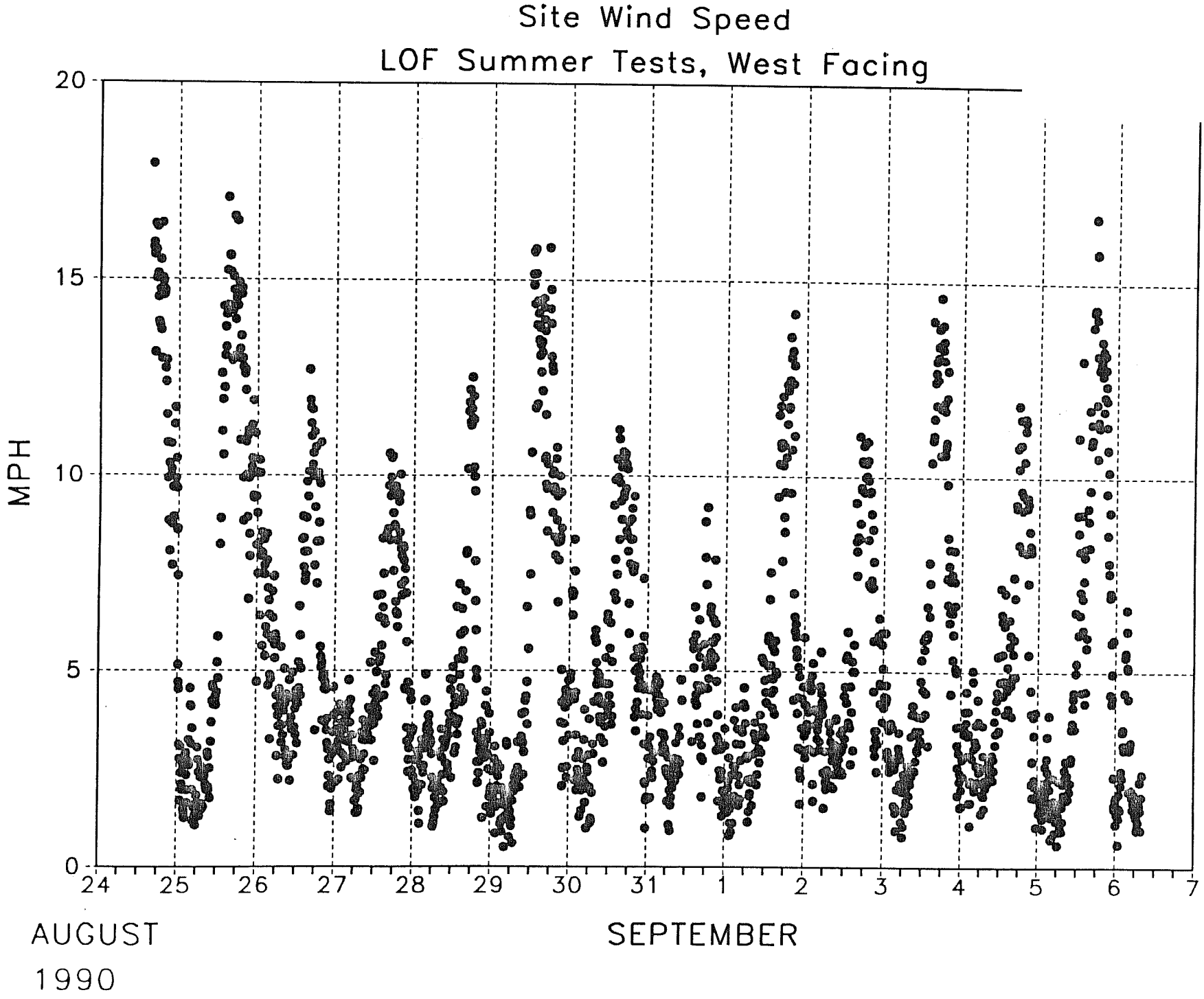
Site Wind Speed
LOF Summer Tests, West Facing
MPH
20
15
10
5
0
24
25
26
27
28
29
30
31
1
2
3
4
5
6
7
AUGUST
SEPTEMBER
1990

Fig 12

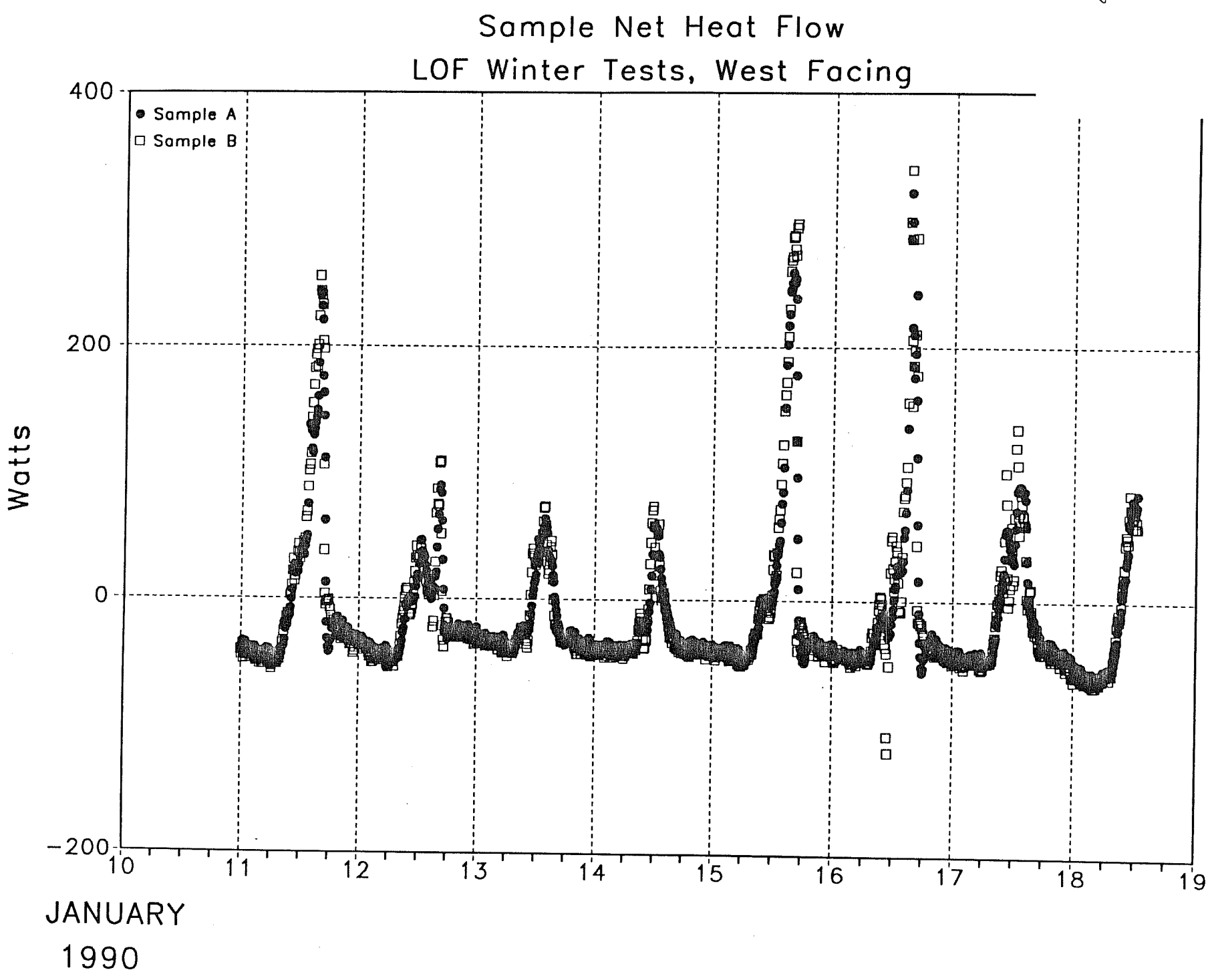

3279158920

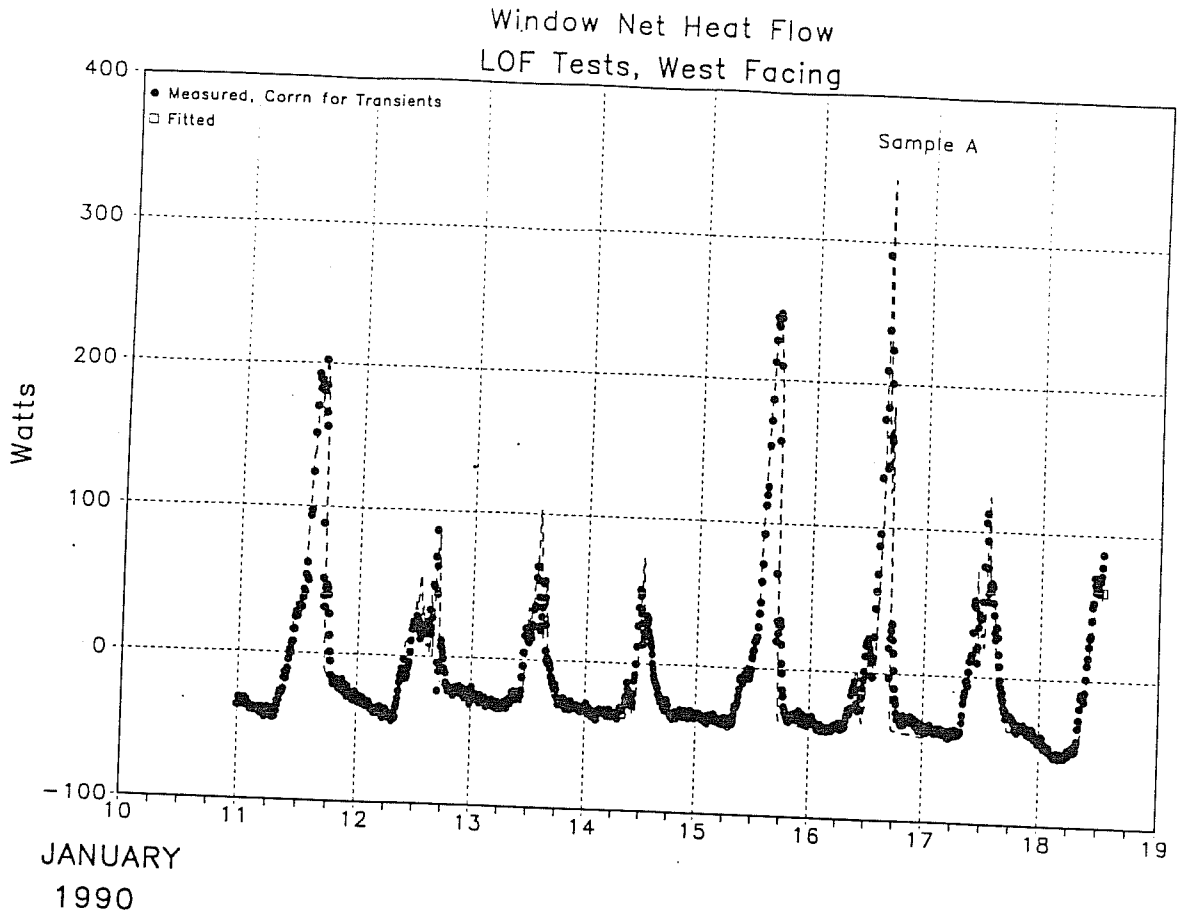

52690261

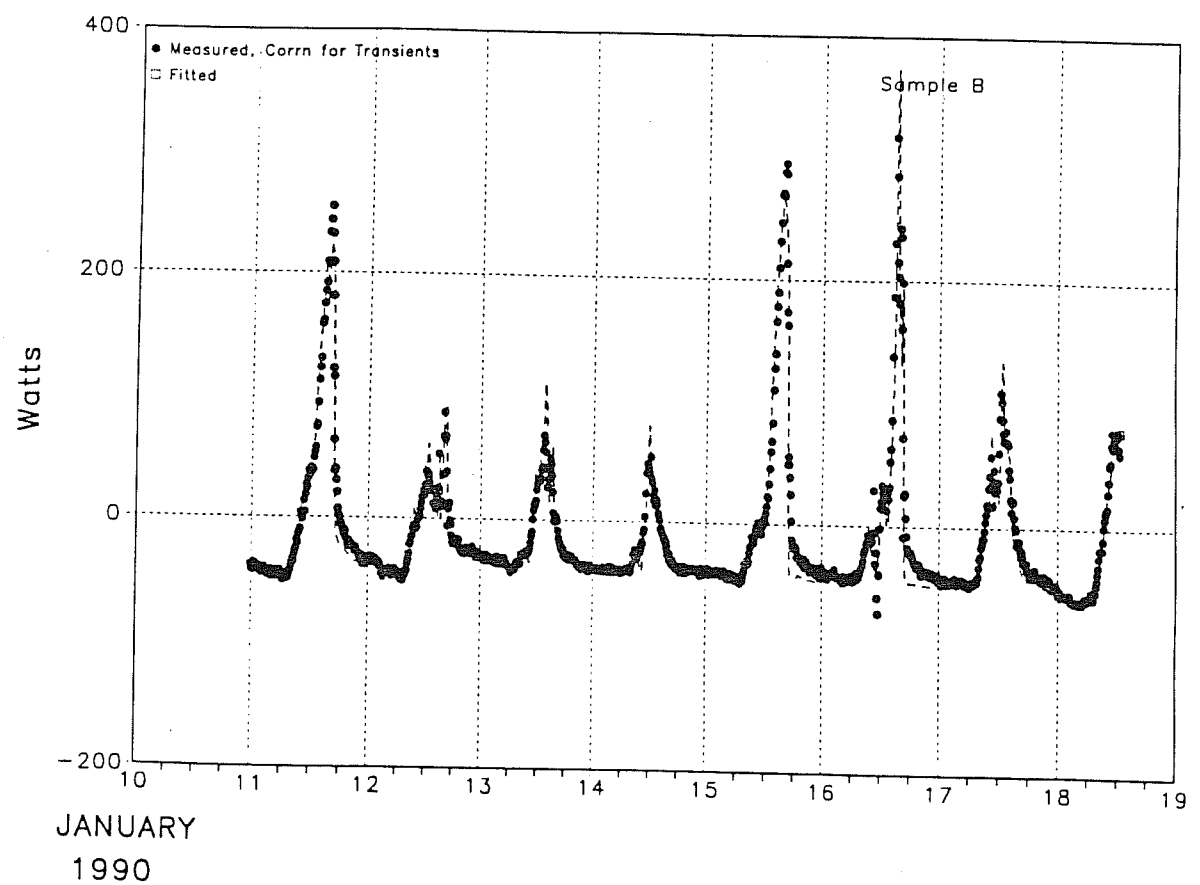

52690261

Fig 13

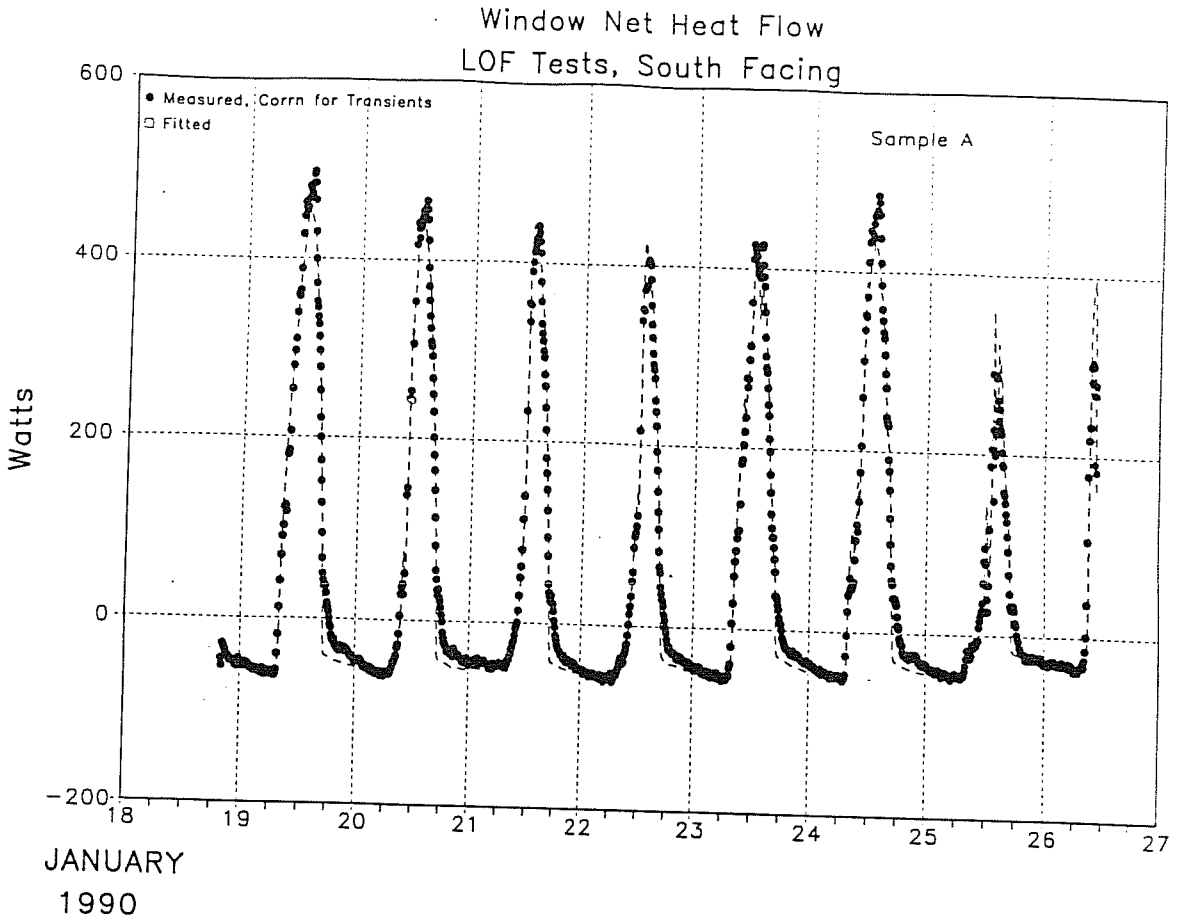

52690261

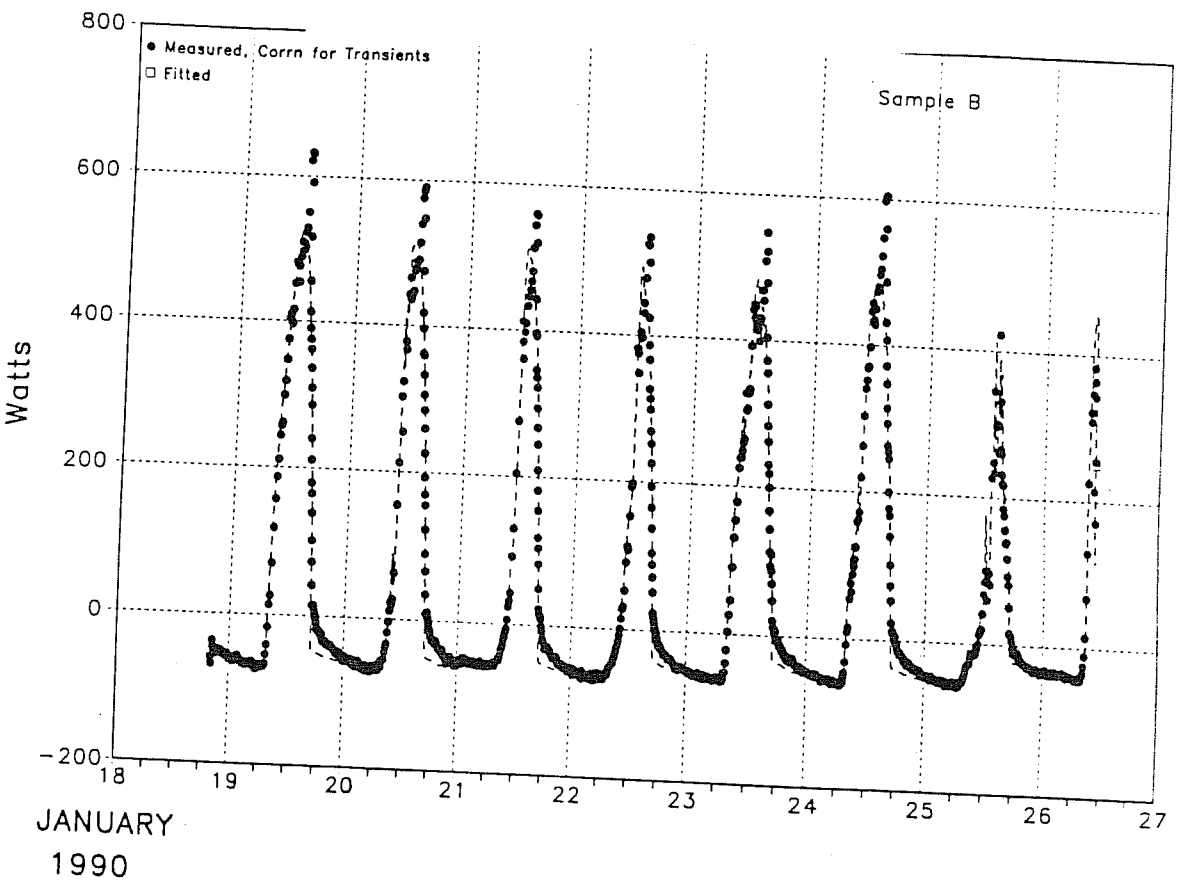

52690261

Fig. 14

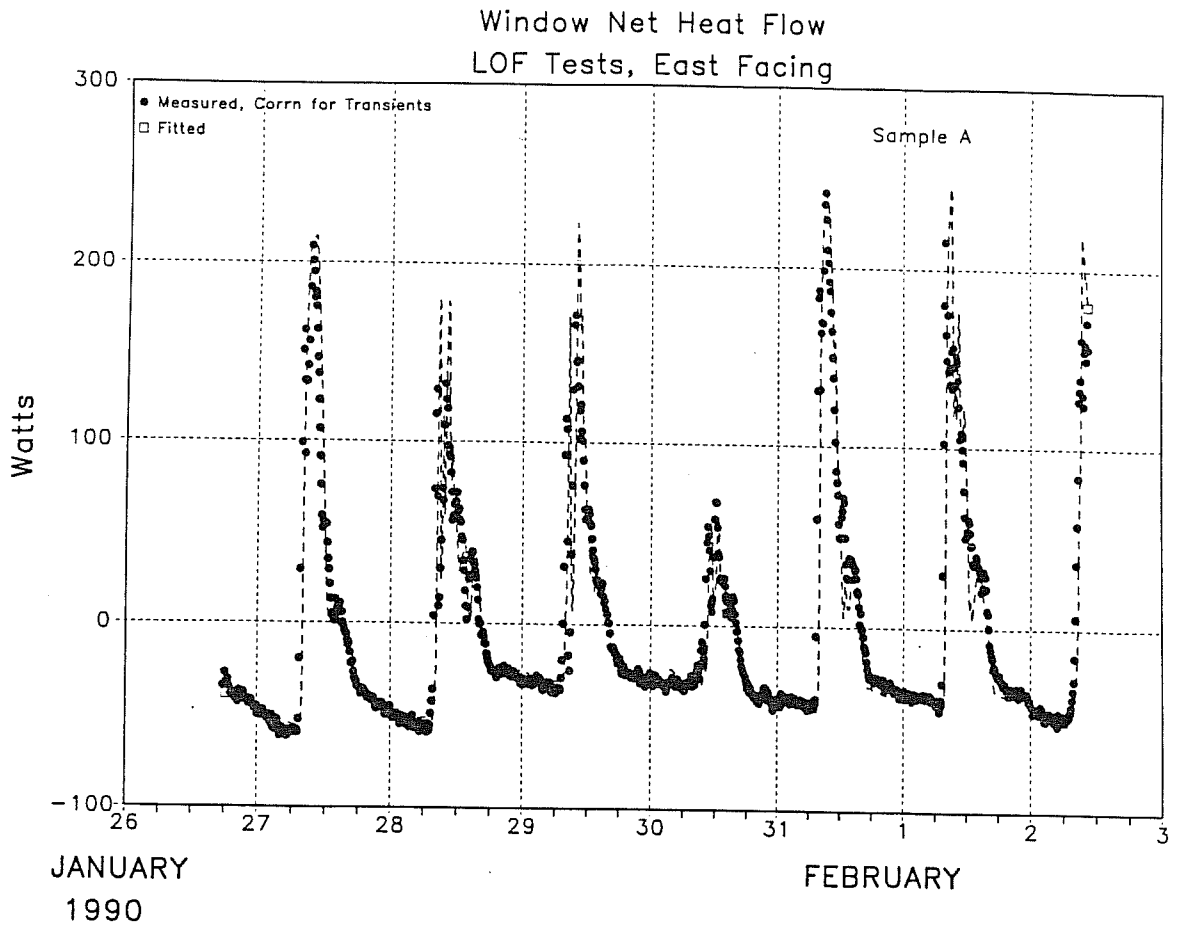
Window Net Heat Flow
LOF Tests, East Facing
Measured, Corrn for Transients
Fitted
Sample A
Watts
300
200
100
0
-100
26
27
28
29
30
31
1
2
3
JANUARY
1990
FEBRUARY
52690261

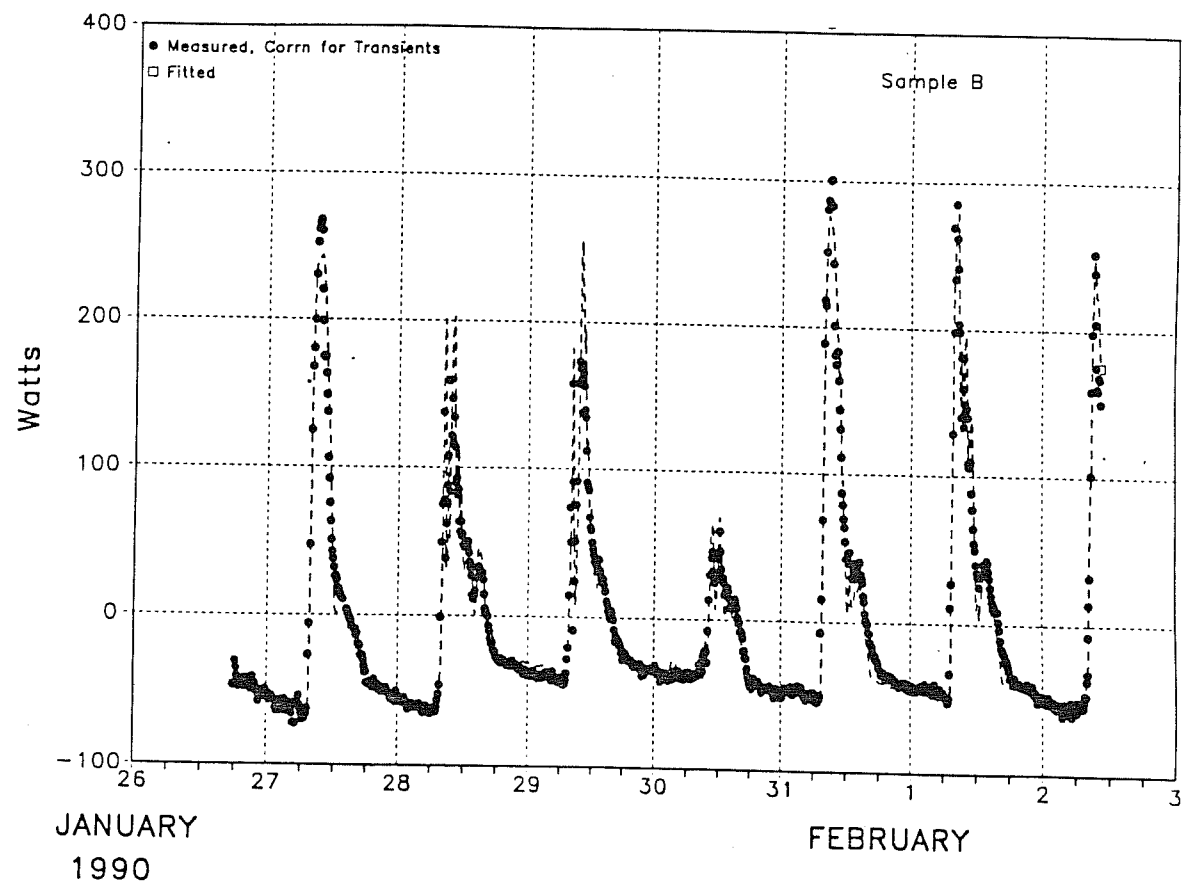
Measured, Corrn for Transients
Fitted
Sample B
Watts
400
300
200
100
0
-100
26
27
28
29
30
31
1
2
3
JANUARY
1990
FEBRUARY
52690261

Fig. 15

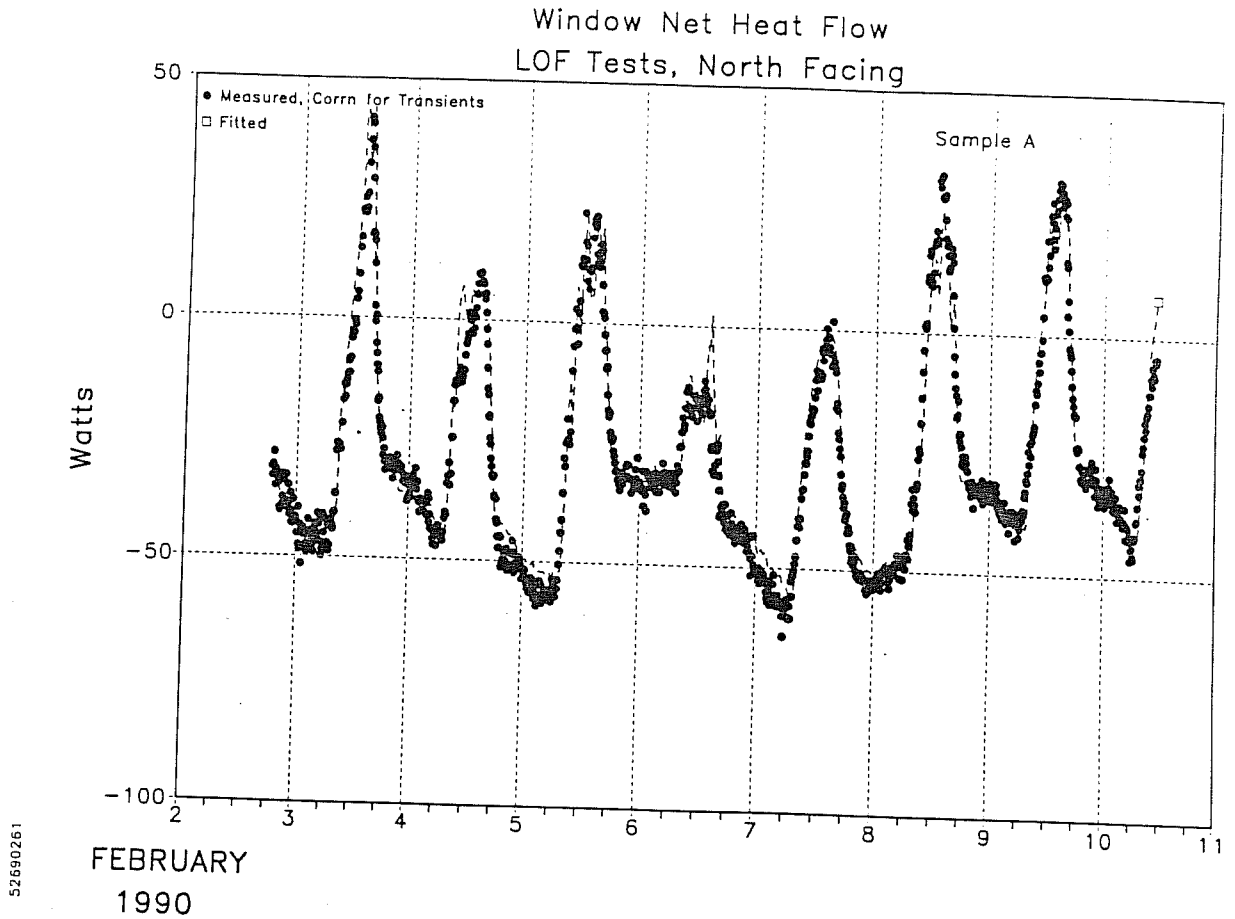
Window Net Heat Flow
LOF Tests, North Facing
Measured, Corrn for Transients
Fitted
Sample A
Watts
50
0
-50
-100
2
3
4
5
6
7
8
9
10
11
FEBRUARY
1990
52690261

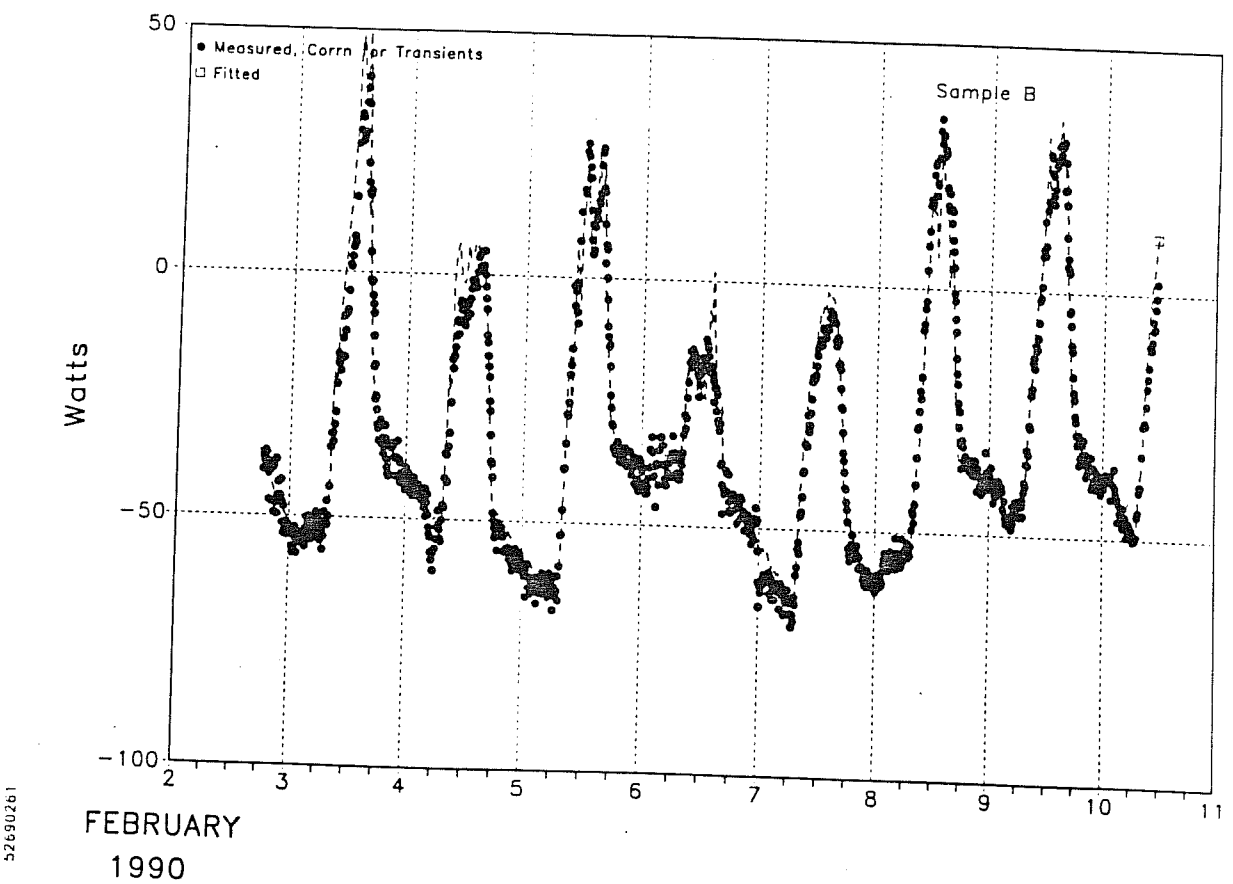
Measured, Corrn for Transients
Fitted
Sample B
Watts
50
0
-50
-100
2
3
4
5
6
7
8
9
10
11
FEBRUARY
1990
52690261

Fig. 16

Fig 17

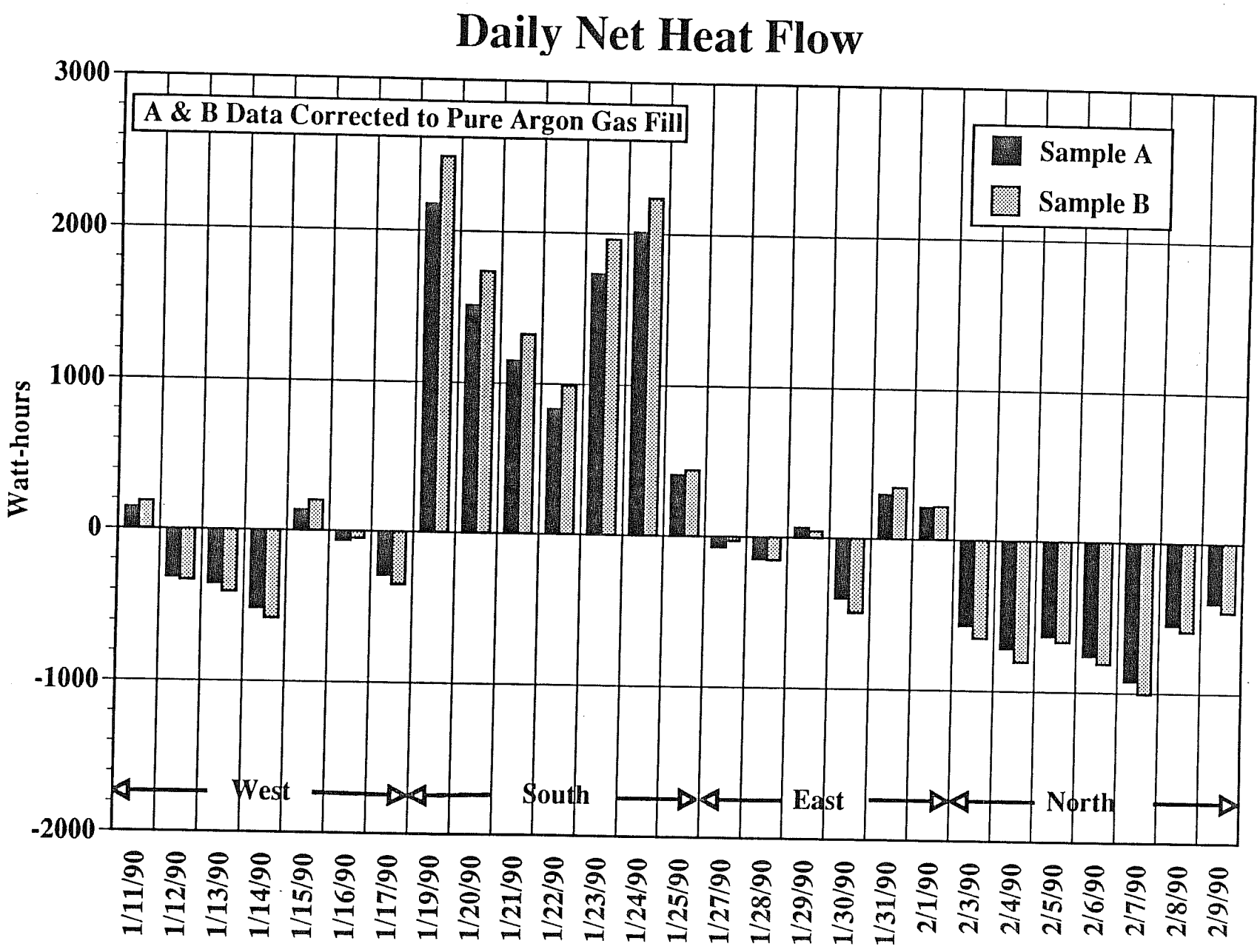
Daily Net Heat Flow
A & B Data Corrected to Pure Argon Gas Fill
Sample A
Sample B
Watt-hours
3000
2000
1000
0
-1000
-2000
West
South
East
North
1/11/90
1/12/90
1/13/90
1/14/90
1/15/90
1/16/90
1/17/90
1/19/90
1/20/90
1/21/90
1/22/90
1/23/90
1/24/90
1/25/90
1/27/90
1/28/90
1/29/90
1/30/90
1/31/90
2/1/90
2/3/90
2/4/90
2/5/90
2/6/90
2/7/90
2/8/90
2/9/90

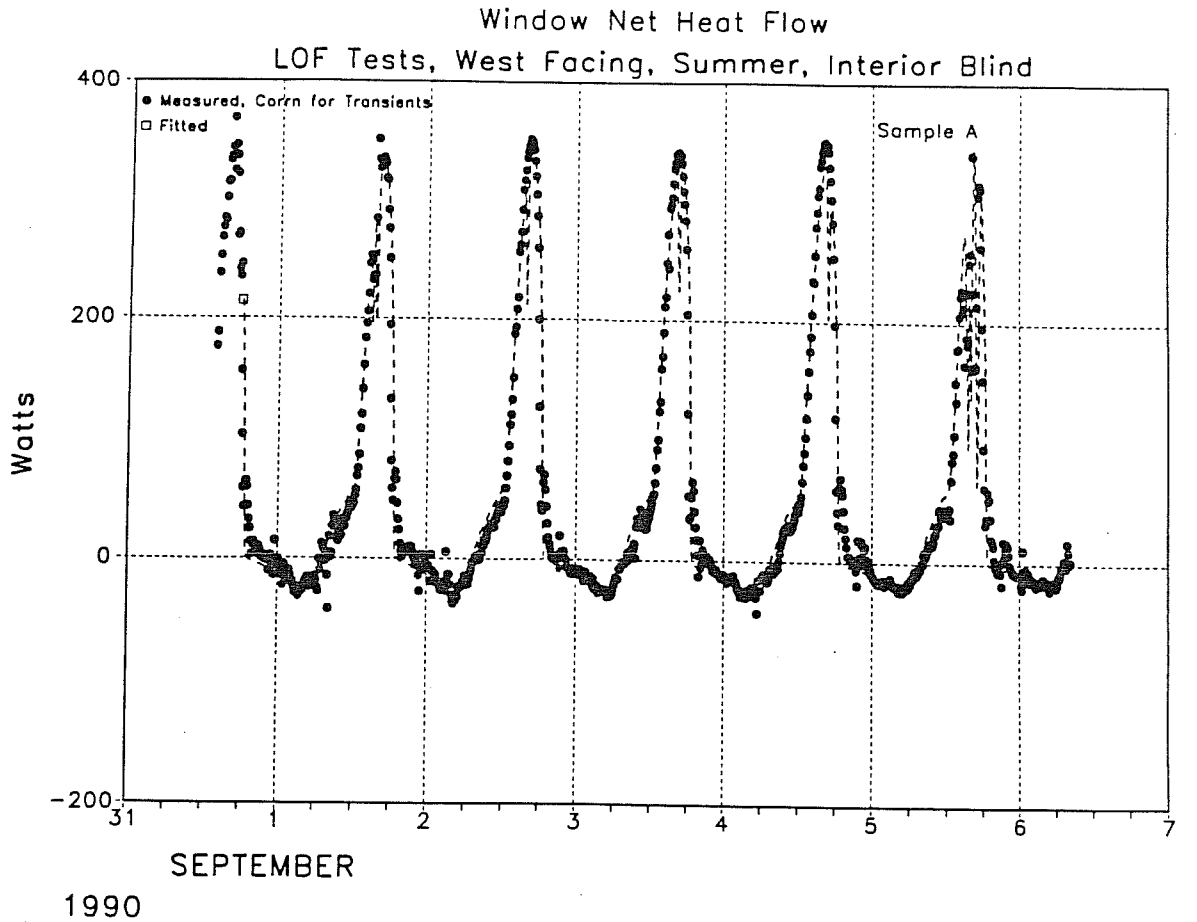

4089159048

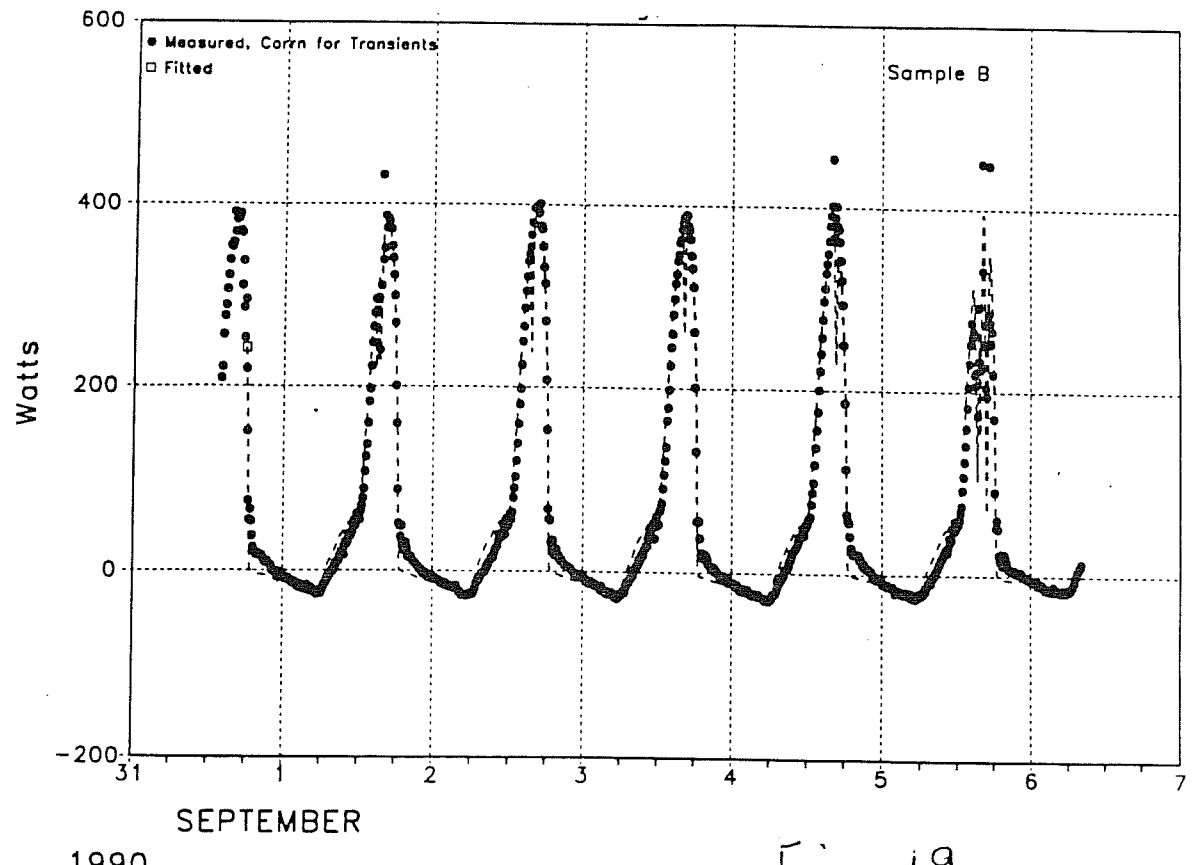

4089159048

Fig. 19

Fig 20

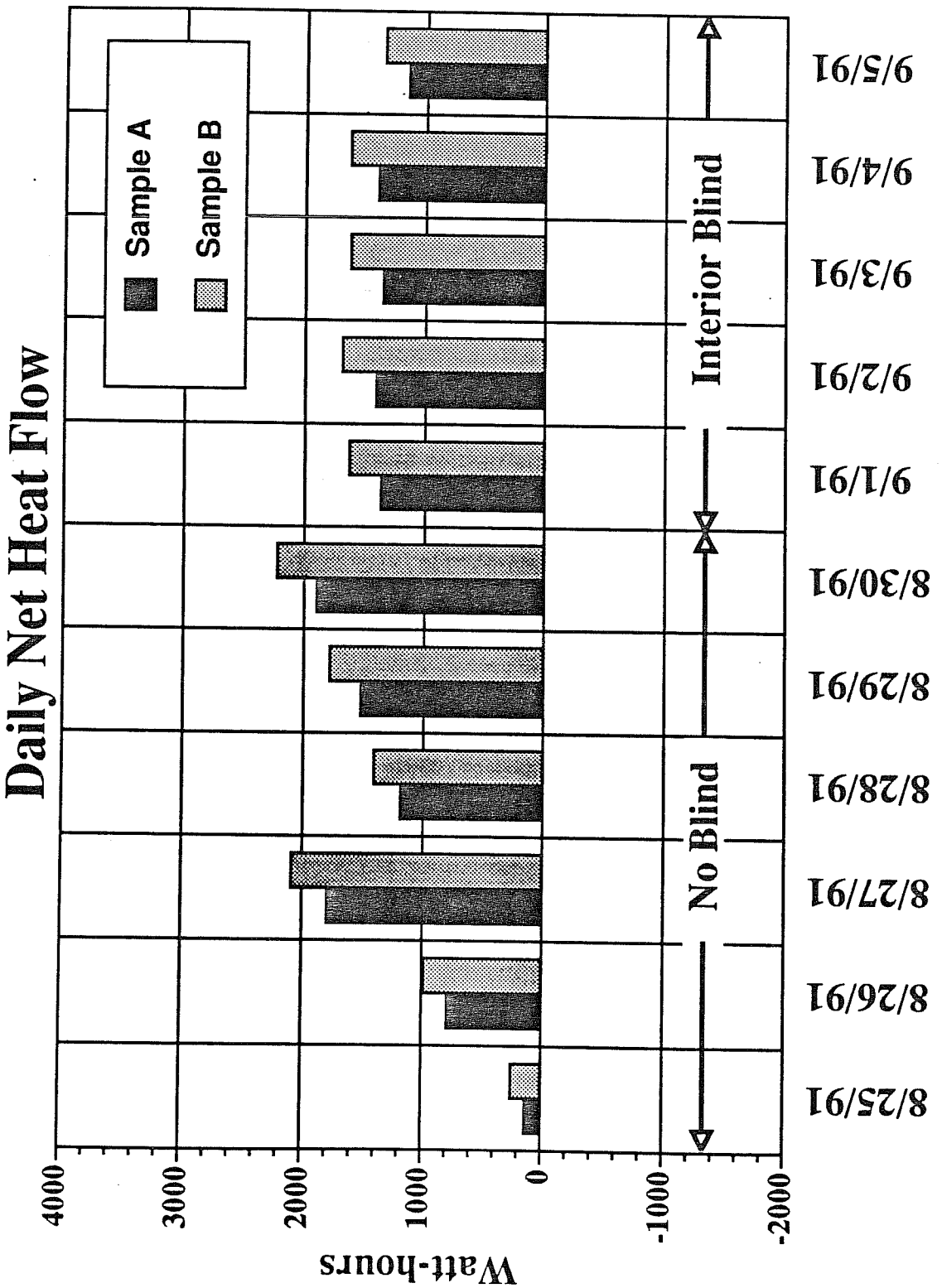
Daily Net Heat Flow
Sample A
Sample B
Watt-hours
4000
3000
2000
1000
0
-1000
-2000
No Blind
Interior Blind
8/25/91
8/26/91
8/27/91
8/28/91
8/29/91
8/30/91
9/1/91
9/2/91
9/3/91
9/4/91
9/5/91

Fig 21

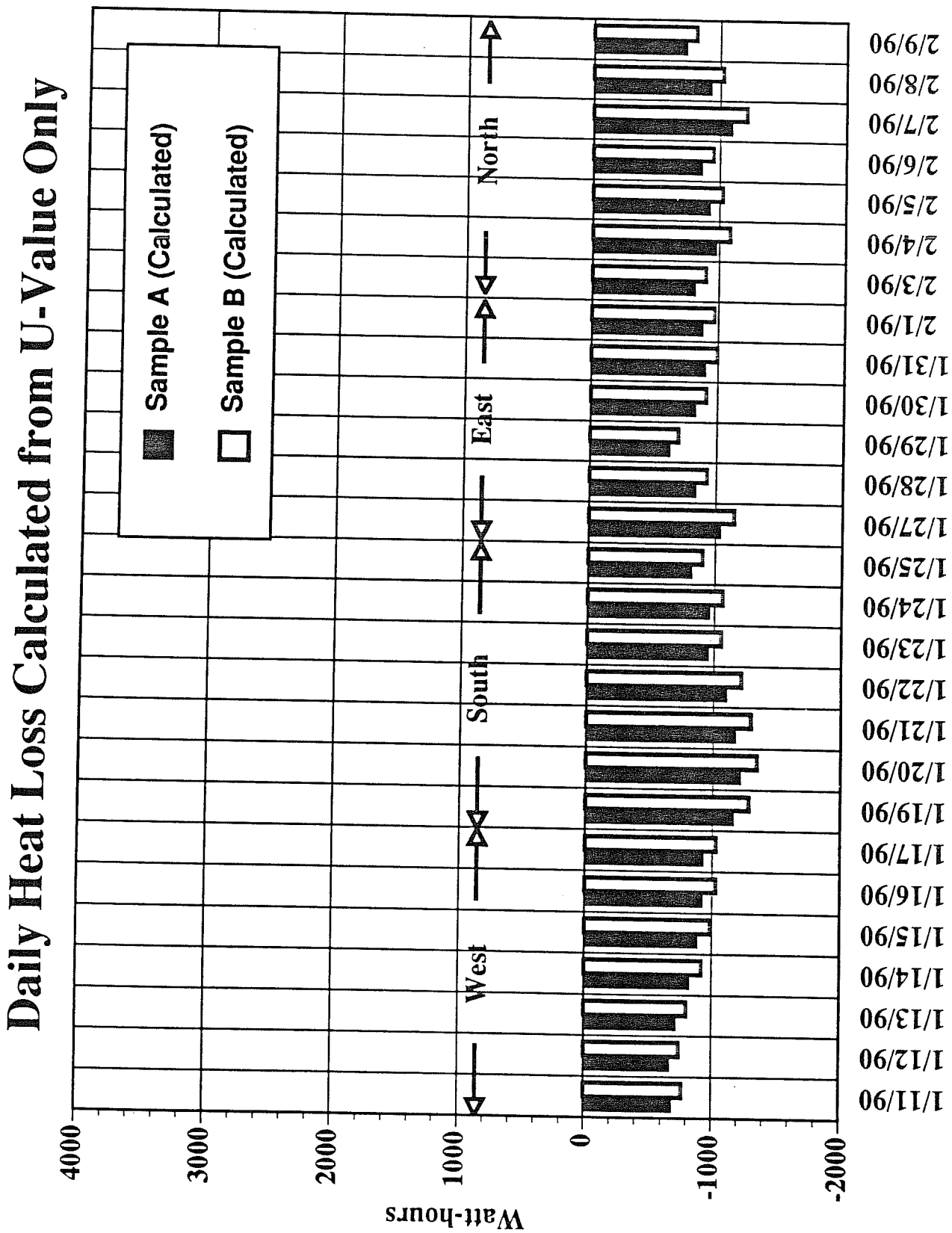
Daily Heat Loss Calculated from U-Value Only
Sample A (Calculated)
Sample B (Calculated)
West
South
East
North
Watt-hours
4000
3000
2000
1000
0
-1000
-2000
1/11/90
1/12/90
1/13/90
1/14/90
1/15/90
1/16/90
1/17/90
1/19/90
1/20/90
1/21/90
1/22/90
1/23/90
1/24/90
1/25/90
1/27/90
1/28/90
1/29/90
1/30/90
1/31/90
2/1/90
2/3/90
2/4/90
2/5/90
2/6/90
2/7/90
2/8/90
2/9/90

Fig 23

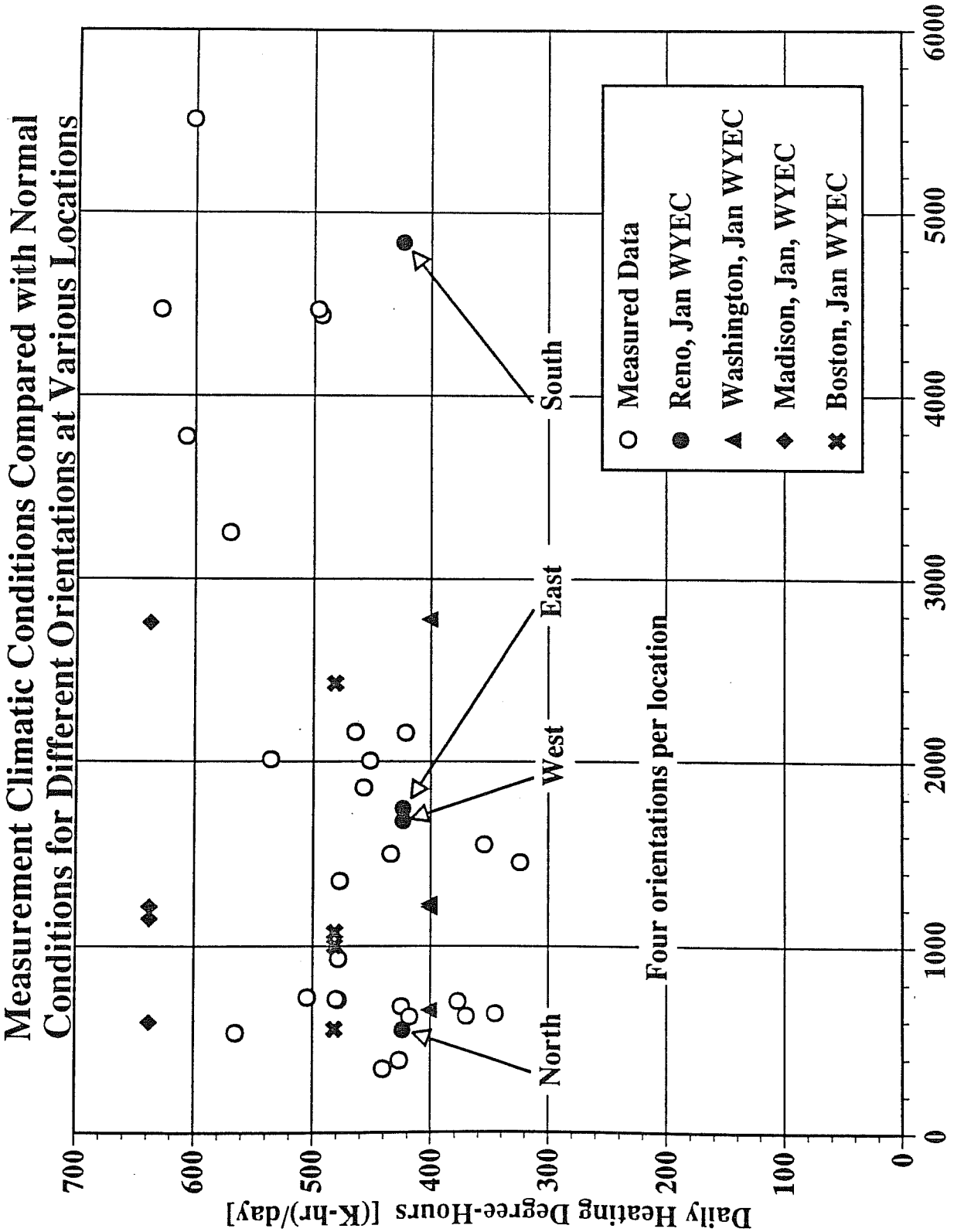
Measurement Climatic Conditions Compared with Normal Conditions for Different Orientations at Various Locations
Daily Heating Degree-Hours [(K-hr)/day]
Daily Vertical-Surface Solar Flux at Window [W-h/(day m**2)]
0
100
200
300
400
500
600
700
0
1000
2000
3000
4000
5000
6000
Four orientations per location
North
West
East
South
Measured Data
Reno, Jan WYEC
Washington, Jan WYEC
Madison, Jan, WYEC
Boston, Jan WYEC